Inorganic Chemistry

Article

pubs.acs.org/IC

Synthesis, Protonation, and Reduction of Ruthenium–Peroxo Complexes with Pendent Nitrogen Bases

Tristan A. Tronic, Werner Kaminsky, Michael K. Coggins, and James M. Mayer*

Department of Chemistry, University of Washington, Box 351700, Seattle, Washington 98195-1700, United States

Supporting Information

ABSTRACT: Cyclopentadienyl and pentamethylcyclopentadienyl ruthenium(II) complexes have been synthesized with cyclic $(RPCH_2NR'CH_2)_2$ ligands, with the goal of using these $[Cp^{R''}Ru(P^R{}_2N^{R'}{}_2)]^+$ complexes for catalytic O_2 reduction to H_2O (R = *t*-butyl, phenyl; R′ = benzyl, phenyl; R″ = methyl, H). In each compound, the Ru is coordinated to the two phosphines, positioning the amines of the ligand in the second coordination sphere where they may act as proton relays to a bound dioxygen ligand. The phosphine, amine, and cyclopentadienyl substituents have been systematically varied in order to understand the effects of each of these parameters on the properties of the complexes. These $Cp^{R''}Ru(P^R{}_2N^{R'}{}_2)^+$ complexes react with O_2 to form η^2-peroxo complexes, which have been characterized by NMR, IR, and X-ray crystallography. The peak reduction potentials of the O_2 ligated complexes have been shown by cyclic voltammetry to vary as much as 0.1 V upon varying the phosphine and amine. In the presence of acid, protonation of these complexes occurs at the pendent amine, forming a hydrogen bond between the protonated amine and the bound O_2. The ruthenium–peroxo complexes decompose upon reduction, precluding catalytic O_2 reduction. The irreversible reduction potentials of the protonated O_2 complexes depend on the basicity of the pendent amine, giving insight into the role of the proton relay in facilitating reduction.

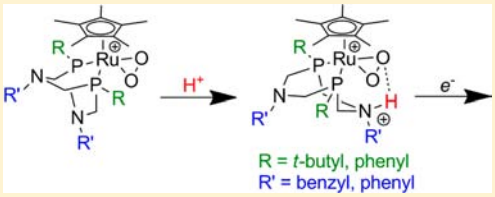

INTRODUCTION

The efficient reduction of dioxygen to water is critical to the development of hydrogen as a fuel source, as this is the cathodic half-reaction in a polymer electrolyte membrane (PEM) fuel cell.[1−3] This reaction, termed the oxygen reduction reaction (ORR), is a proton-coupled electron transfer (PCET) process, requiring the coordinated movement of four electrons and four protons per molecule of O_2. An ideal catalyst would control the delivery of these electrons and protons and would stabilize the many intermediates in this process.[4,5] The extensive research in this area has primarily focused on using redox-active transition metal complexes to control the electron delivery. Much progress has been made by studying iron,[6−8] cobalt,[9−11] and copper[12−15] complexes with primary coordination spheres that resemble the active sites of biological oxidase enzymes.[16−18] In one recent elegant example, Collman, Chidsey, and co-workers have attached ORR catalysts to a gold electrode via a self-assembled monolayer (SAM), and length of the SAM was varied to control the rate of electron transfer to the catalyst.[19] In contrast to the considerable progress that has been made in controlling electron delivery, only recently have complexes been developed that attempt to control the delivery of protons.[20−25] This report focuses on developing an understanding of the design requirements for a catalyst to control the delivery of protons to O_2-derived substrates, using amine bases in the second coordination sphere that can act as proton relays.[26,27]

The utility of positioned proton relays in molecular, transition metal-catalyzed redox transformations of small molecules has been extensively demonstrated for H_2 oxidation/H^+ reduction with complexes of Fe,[28−30] Ni,[26,31−37] and Co.[38−40] In particular, 1,5-diaza-3,7-diphosphacyclooctane $(P^R{}_2N^{R'}{}_2)$ ligands have emerged as powerful ligands for H_2 oxidation/H^+ reduction catalysts,[26,29,32−34,39,40] in part because they bind to the metal center preferentially through the phosphines, and their semirigid cyclooctane structure prevents amine binding to the metal center but positions the amines near the site of H_2 binding/formation. Additionally, substitution of the R and R′ groups of these ligands is relatively synthetically facile and allows for tuning of the metal's redox properties and pendent amine basicity. The $P^R{}_2N^{R'}{}_2$ ligands have been shown to dramatically improve catalyst overpotential and turnover frequency in these systems. Recently, there has been considerable interest in extending the utility of these ligands to proton-coupled redox transformations of other small molecules including CO_2/HCOOH[41,42] and N_2/NH_3.[43,44]

The utility of acidic proton relays in O_2 reduction has been explored previously with carboxylic acids rather than amines as proton relays. Nocera and co-workers have pioneered the use of proton relays with their "hangman" porphyrinoid complexes, which position a carboxylic acid rigidly above the metal center.[22,23] They have shown with a cobalt "hangman" porphyrin complex, selectivity for H_2O production can be increased from 48% to 71% in electronically similar complexes.[22] We have built on this work, showing that, with

Received: June 28, 2012
Published: October 4, 2012

a series of iron (*meso*-tetra(carboxyphenyl))porphine catalysts, positioning carboxylic acids near the oxygen binding site of the complex dramatically improves catalyst stability and product selectivity.[25] While changes to the electronic structure of these catalysts have been explored, no systematic study of the pK_a of the proton relay has been performed, nor has the mechanistic role of the proton relay been elucidated in these systems. We and others have begun exploring the use of $P^R_2N^{R'}_2$ ligands for O_2 reduction, motivated in part by the relative synthetic ease with which the pendent base may be modified without significant changes to ligand structure. Yang et al. have demonstrated that Ni($P^R_2N^{R'}_2$) complexes can reduce O_2 to H_2O if a sufficiently basic pendent amine is used.[45] However, this system was not stable under catalytic conditions, and no mechanistic data could be obtained. To address this lack of mechanistic information, we have explored Ru complexes with $P^R_2N^{R'}_2$ ligands as potentially more stable systems, and recently we have reported the synthesis and protonation of a $[Cp^*Ru(P^R_2N^{R'}_2)]^+$ (Cp^* = η^5-C_5Me_5) complex that binds O_2.[46]

The previously reported complex $[Cp^*Ru(P^{tBu}_2N^{Bn}_2)]^+$ (tBu = *t*-butyl, Bn = benzyl) reacts with O_2 to make an η^2-peroxo complex.[46] In the presence of acid, $[Cp^*Ru(P^{tBu}_2N^{Bn}_2)(O_2)]^+$ is protonated at a pendent amine, forming a hydrogen bond with the O_2 ligand. Both the protonated and unprotonated species were characterized by X-ray crystallography, allowing the interaction between the protonated pendent amine and the O_2 to be visualized. This species demonstrated a proton dependent reduction potential, suggestive that the pendent amine may be able to relay protons to the O_2, but the reduction mechanism could not be determined.

We have sought better mechanistic understanding of the ability of these complexes to direct protons to O_2 during reduction by studying the effects of variations in the ligands. Presented herein are the synthesis, protonation, and reduction of new $[Cp^{R''}Ru(P^R_2N^{R'}_2)(O_2)]^+$ complexes with systematic variation in the ligands from the previously communicated $P^{tBu}_2N^{Bn}_2$ complex. A less basic pendent amine has been tested by synthesizing a complex with a $P^{tBu}_2N^{Ph}_2$ ligand (Ph = phenyl), and a less electron donating phosphine has been tested by synthesizing a complex with a $P^{Ph}_2N^{Bn}_2$ ligand. Additionally, the role of the Cp* has been tested by substituting this for a Cp ligand (Cp = η^5-C_5H_5). The effect of each of these changes on the basicity and reduction potential of the complex has been probed. These studies have shown that these complexes decompose during reduction, likely due to oxidation of the phosphines, highlighting the limitations of applying $P^R_2N^{R'}_2$ ligands to O_2 reduction. The studies have also shown that the potential for reduction of these species can be controlled via the acidity of the pendent amine, highlighting the important role that proton relays can play in improving O_2 reduction catalysts.

RESULTS

Synthesis of Cp*Ru($P^R_2N^{R'}_2$)Cl and Related Complexes. New complexes of Cp*Ru(II) with 1,5-diaza-3,7-diphosphacyclooctane ($P^R_2N^{R'}_2$) ligands were synthesized by reaction of $Cp^*Ru^{II}Cl$ precursors with the appropriate $P^R_2N^{R'}_2$ ligand (Scheme 1), similar to the synthesis of Cp*Ru($P^{tBu}_2N^{Bn}_2$)Cl reported in the previous communication.[46] Cp*Ru($P^{tBu}_2N^{Ph}_2$)Cl was prepared by the room temperature reaction of $[Cp^*RuCl]_4$ with $P^{tBu}_2N^{Ph}_2$ in THF. The reaction is slow, due to the low solubility of $P^{tBu}_2N^{Ph}_2$ in THF, but after three days affords the desired product in modest yield as an orange powder. The same synthetic procedure with $P^{Ph}_2N^{Bn}_2$ gave a mixture of Cp*Ru($P^{Ph}_2N^{Bn}_2$)Cl and other products, as determined by NMR, that could not be separated by recrystallization or column chromatography. These side products may contain diphosphine ligands that bridge multiple Ru centers, as has been observed in the synthesis of Cp*Ru(dppm)Cl.[47] In this case, phosphine ligand exchange is a better procedure: refluxing $Cp^*Ru(PPh_3)_2Cl$ with $P^{Ph}_2N^{Bn}_2$ in toluene for two days gave Cp*Ru($P^{Ph}_2N^{Bn}_2$)Cl as a yellow powder in modest yield.

Scheme 1. Synthesis of Chloride Complexes

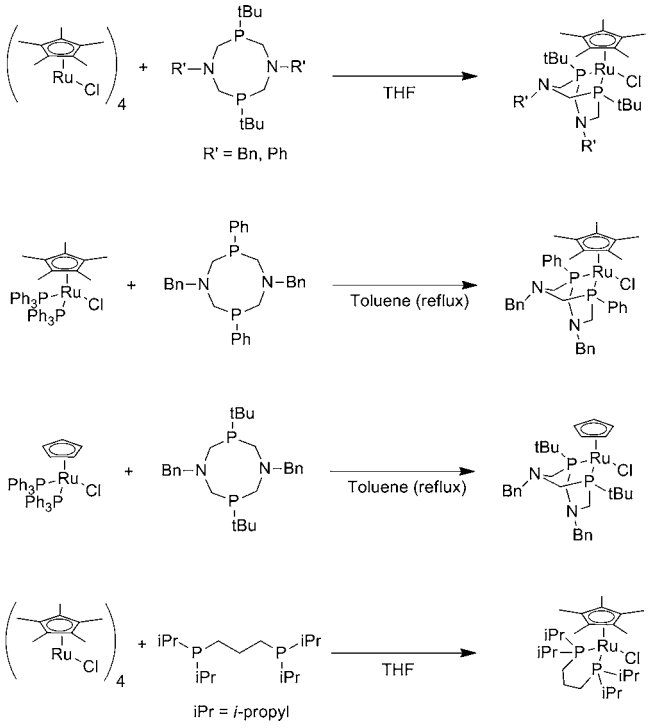

The Cp*Ru($P^R_2N^{R'}_2$)Cl compounds have been characterized by ^{1}H and ^{31}P NMR spectroscopy and X-ray crystallography. Their ^{31}P NMR spectra contain only one sharp singlet corresponding to the two equivalent phosphines. The X-ray crystal structures show that the $P^R_2N^{R'}_2$ ligands bind only through the phosphines, with the third leg of the piano stool occupied by a bound Cl^- (Figure 1a,b; the structure of Cp*Ru($P^{tBu}_2N^{Bn}_2$)Cl is reported in ref 46). The nitrogen bases in each complex are positioned in the second coordination sphere of the metal. The lone pair of the nitrogen closest to the Cl^- (N1) points away from electron-rich Cl^-, and the lone pair of N2 points away from the lone pair of N1. The binding of the phosphine ligands is essentially the same in Cp*Ru($P^{tBu}_2N^{Bn}_2$)-Cl[46] and Cp*Ru($P^{tBu}_2N^{Ph}_2$)Cl, with average Ru–P distances of 2.309 ± 0.004 Å and 2.304 ± 0.009 Å and average P–Ru–P angles of 78.0 ± 0.1° and 78.4 ± 0.1°, respectively (avg of two independent molecules in each unit cell). With a phenyl substituent on the phosphine (Cp*Ru($P^{Ph}_2N^{Bn}_2$)Cl), the average Ru–P bond distance is shortened by 0.063 ± 0.005 Å (Table 1).

The Cp derivative CpRu($P^{tBu}_2N^{Bn}_2$)Cl was obtained in good yield by refluxing $CpRu(PPh_3)_2Cl$ with $P^{tBu}_2N^{Bn}_2$ in toluene for two days. Its ^{1}H NMR spectrum closely resembles that of Cp*Ru($P^{tBu}_2N^{Bn}_2$)Cl, and it has a $^{31}P\{^1H\}$ NMR singlet resonance that is 11.8 ppm downfield from that of Cp*Ru-($P^{tBu}_2N^{Bn}_2$)Cl (Table 2). CpRu($P^{tBu}_2N^{Bn}_2$)Cl did not form

dx.doi.org/10.1021/ic3013987 | *Inorg. Chem.* 2012, 51, 10916–10928

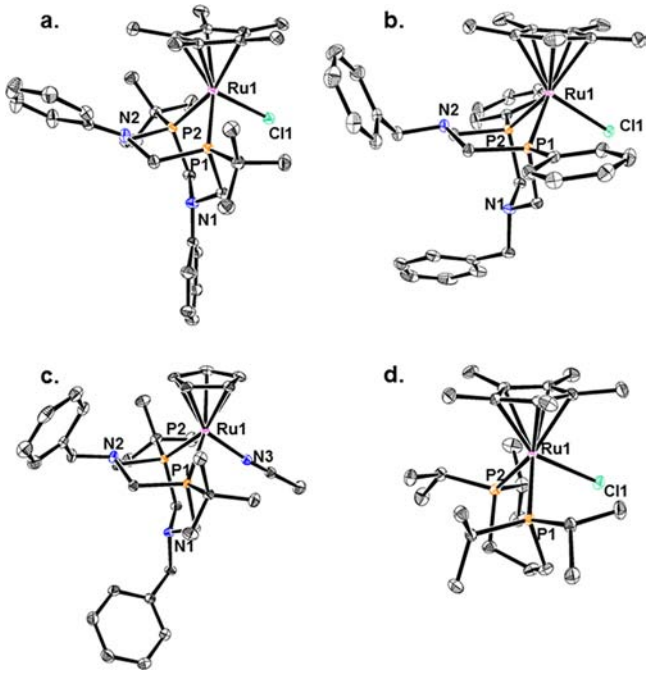

Figure 1. ORTEPs of (a) Cp*Ru($P^{tBu}_2N^{Ph}_2$)Cl, (b) Cp*Ru($P^{Ph}_2N^{Bn}_2$)Cl, (c) [CpRu($P^{tBu}_2N^{Bn}_2$)(MeCN)][PF_6], and (d) Cp*Ru(dippp)Cl. Thermal ellipsoids are shown at 50% probability. Hydrogen atoms and solvent molecules have been omitted for clarity. Only the cationic portion of [CpRu($P^{tBu}_2N^{Bn}_2$)(MeCN)][PF_6] and only one of the two independent molecules of Cp*Ru($P^{tBu}_2N^{Ph}_2$)Cl in the unit cell are shown.

crystals suitable for X-ray diffraction. However, an X-ray structure was obtained for a related complex with acetonitrile in place of chloride, [CpRu($P^{tBu}_2N^{Bn}_2$)(MeCN)][PF_6], synthesized by chloride abstraction with $TlPF_6$ in the presence of acetonitrile. The geometry of the phosphine ligand of this acetonitrile complex closely resembles that of the Cp*Ru($P^R_2N^{R'}_2$)Cl complexes (Figure 1c).

A closely related Cp*Ru complex without a pendent amine, Cp*Ru(dippp)Cl (dippp =1,3-bis(diisopropylphosphino)-propane), was synthesized for comparison with the ($P^R_2N^{R'}_2$) derivatives. Its X-ray crystal structure (Figure 1d) shows that the bulky isopropyl substituents and trimethylene backbone of dippp resemble the *t*-butyl substituents and three-atom backbone of $P^{tBu}_2N^{Bn}_2$. Although the crystallographically observed Ru−P bond lengths and bite angle are slightly larger in Cp*Ru(dippp)Cl, this complex appears to be a good all-alkyl analogue compared to Cp*Ru($P^{tBu}_2N^{Bn}_2$)Cl based on the reactivity and redox potentials presented below.

Cp*Ru($P^{tBu}_2N^{Bn}_2$)Cl can be protonated, as observed by NMR spectroscopy. Addition of 1 equiv of protonated dimethylformamide triflate ([H^+DMF][OTf], pK_a in acetonitrile of 6.1),[48] to a solution of Cp*Ru($P^{tBu}_2N^{Bn}_2$)Cl in CD_2Cl_2 formed a single new species by ^{1}H and ^{31}P NMR spectroscopies. In the ^{1}H NMR spectrum of Cp*Ru($P^{tBu}_2N^{Bn}_2$)Cl + [H^+DMF][OTf], one of the benzyl CH_2 resonances is shifted downfield and split into a doublet (J_{H-H} = 5.5 Hz) due to its proximity to the acidic N*H*. The N*H* proton appears as a broad singlet at 11.1 ppm. The ^{1}H NMR spectrum of this solution closely resembles that of the protonated O_2 complex [Cp*Ru($P^{tBu}_2N^{Bn}_2H$)(O_2)][PF_6] (see Supporting Information).[46] This suggests that protonation of the chloride species in CD_2Cl_2 is similar to protonation of the O_2 species, with the acidic proton located on the pendent amine (see below).

Synthesis of Dioxygen Complexes. Dioxygen-bound complexes are obtained by chloride abstraction from Cp*Ru($P^R_2N^{R'}_2$)Cl with TlX (X = OTf^- or PF_6^-) in CH_2Cl_2 or acetone solutions open to air (eq 1). These reactions parallel well-known analogues with simple bis(phosphine) ligands,[49] and the chemistry of the dippp complexes is very similar. The O_2 complexes are stable species, and removal of the solvent under vacuum yields [Cp*Ru($P^R_2N^{R'}_2$)(O_2)][X] or [Cp*Ru(dippp)(O_2)][X] as brown solids in high yield. Additionally,

Table 1. Selected Bond Lengths and Angles of Chloride, Acetonitrile, and Dioxygen Ligated Complexes[a]

	P1−Ru1	P2−Ru1	Cl1−Ru1	O1−Ru1	O2−Ru1	O1−O2	P1−Ru1−P2
Cp*Ru($P^{tBu}_2N^{Ph}_2$)Cl[b]	2.3077(4), 2.3043(4)	2.3001(4), 2.3134(4)	2.4597(4), 2.4550(4)				78.272(15), 78.375(15)
Cp*Ru($P^{Ph}_2N^{Bn}_2$)Cl	2.2492(4)	2.2435(4)	2.4412(3)				77.780(12)
[CpRu($P^{tBu}_2N^{Bn}_2$)(MeCN)][PF_6]	2.2868(4)	2.2914(4)					79.643(12)
Cp*Ru(dippp)Cl	2.3271(3)	2.3271(3)	2.4608(3)				88.045(10)
[Cp*Ru($P^{tBu}_2N^{Ph}_2$)Cl][PF_6][b]	2.3758(6), 2.3674(6)	2.3658(5), 2.3759(6)	2.3221(5), 2.3326(5)				77.388(18), 77.511(19)
[Cp*Ru($P^{tBu}_2N^{Bn}_2$)(O_2)][BPh_4][c]	2.3591(3)	2.3668(3)		2.0229(7)	2.0190(7)	1.4009(11)	76.572(9)
[Cp*Ru($P^{tBu}_2N^{Ph}_2$)(O_2)][BPh_4]	2.3660(3)	2.3774(3)		2.0280(8)	2.0227(8)	1.4063(13)	76.957(10)
[Cp*Ru($P^{Ph}_2N^{Bn}_2$) (O_2)][OTf]	2.3053(8)	2.3022(8)		2.028(2)	2.027(2)	1.400(3)	76.83(3)
[CpRu($P^{tBu}_2N^{Bn}_2$)(O_2)][OTf]	2.3264(9)	2.3286(9)		2.027(2)	2.025(3)	1.404(4)	78.59(3)
[Cp*Ru(dippp)(O_2)][PF_6][b]	2.3777(3), 2.3865(3)	2.3812(3), 2.3920(3)		2.0244(10), 2.0312(9)	2.0294(8), 2.0245(8)	1.4003(12), 1.4064(12)	85.524(11), 85.030(10)
[Cp*Ru($P^{tBu}_2N^{Bn}_2H$)(O_2)][PF_6]$_2$[c,d]	2.3574(5), 2.3580(4)	2.3674(5), 2.3744(4)		2.0393(14), 2.0260(11)	2.0362(14), 2.0350(11)	1.405(2), 1.4161(17)	78.412(16), 78.093(14)
[Cp*Ru($P^{Ph}_2N^{Bn}_2H$)(O_2)][OTf]$_2$	2.2974(9)	2.3224(9)		2.025(2)	2.041(2)	1.414(4)	78.46(4)

[a]Distances are in Å, angles are in deg. [b]Values are given for each independent molecule within the unit cell. [c]Reference 46. [d]Values are given for the two different crystal structures obtained of this material (see ref 46).

dx.doi.org/10.1021/ic3013987 | *Inorg. Chem.* 2012, 51, 10916−10928

Table 2. Selected ^{1}H and ^{31}P{^{1}H} NMR Resonances and ν(O−O)[a]

compd	^{31}P{^{1}H}	^{1}H(C_5CH_3)$_5$	^{1}H(NH^+)	ν(O−O) [ν(^{18}O−^{18}O)]
Cp*Ru($P^{tBu}_2N^{Bn}_2$)Cl[a]	40.0	1.62		
Cp*Ru($P^{Ph}_2N^{Bn}_2$)Cl	31.0	1.29		
Cp*Ru($P^{tBu}_2N^{Ph}_2$)Cl	44.0	1.68		
CpRu($P^{tBu}_2N^{Bn}_2$)Cl	51.8	4.64 (C_5H_5)		
Cp*Ru(dippp)Cl	32.5	1.63		
[Cp*Ru($P^{tBu}_2N^{Bn}_2$)(O_2)][PF_6][b]	29.4	1.72		935 [880]
[Cp*Ru($P^{Ph}_2N^{Bn}_2$)(O_2)][OTf]	22.0	1.25		926 [879]
[Cp*Ru($P^{tBu}_2N^{Ph}_2$)(O_2)][OTf]	30.2	1.82		930 [880]
[CpRu($P^{tBu}_2N^{Bn}_2$)(O_2)][OTf]	45.9	5.83 (C_5H_5)		*d*
[Cp*Ru(dippp)(O_2)][PF_6]	23.3	1.77		*d*
[Cp*Ru($P^{tBu}_2N^{Bn}_2H$)(O_2)][PF_6]$_2$[b]	30.3[c]	1.81	7.68	905 [840]
[Cp*Ru($P^{Ph}_2N^{Bn}_2H$)(O_2)][PF_6]$_2$	16.6	1.24	8.29	*d*
[Cp*Ru($P^{tBu}_2N^{Ph}_2H$)(O_2)][PF_6]$_2$	41.6	2.01	9.98	~910[e] [857]

[a]Chemical shifts in δ (ppm); ν(O−O) in cm^{-1}. [b]Data from ref 46. [c]Resonance is broad at room temperature. [d]ν(O−O) not assigned. [e]ν(O−O) is obscured by absorbance of the CH_2Cl_2 solvent. An approximate value based on the observed ν(^{18}O−^{18}O) is provided, assuming harmonic oscillator behavior for the O−O bond (see text).

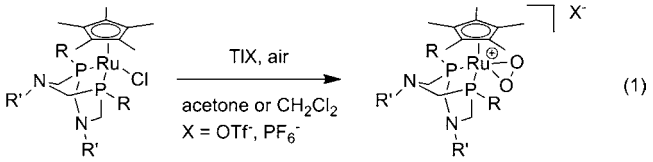

(1)

[Cp*Ru($P^{tBu}_2N^{Ph}_2$)(O_2)]$^+$ and [Cp*Ru(dippp)(O_2)]$^+$ may be obtained as tetraphenylborate (BPh_4^-) salts by stirring the respective Cl$^-$ complex with $NaBPh_4$ in ethanol in the air. The complexes have been characterized by X-ray crystallography and IR spectroscopy, and by their well-resolved ^{1}H and ^{31}P spectra. One sharp singlet is observed in the ^{31}P{^{1}H} spectra due to the equivalent phosphines of the $P^R_2N^{R'}_2$ ligand, shifted ~10 ppm upfield of the singlet observed for the chloride precursors (Table 2). These peroxo complexes appear to be indefinitely stable in the solid state, and stable for several days in CH_2Cl_2 solution before any decomposition is evident by NMR. In solution they do not lose their O_2 ligand under vacuum or under a nitrogen atmosphere, though the O_2 is displaced by solvent in acetonitrile solution.

The X-ray crystal structures of the [Cp*Ru($P^R_2N^{R'}_2$)(O_2)]$^+$ and [Cp*Ru(dippp)(O_2)]$^+$ complexes show that the O_2 ligand is bound in an η^2-fashion (Figure 2), with O−O bond distances of 1.400−1.406 Å (Table 1). The O−O stretching frequencies were obtained from spectra of KBr pellets and confirmed by $^{18}O_2$-labeling; for instance, a value of 930 cm^{-1} ($\nu_{18O-18O}$ = 880 cm^{-1}) is observed for the $P^{tBu}_2N^{Ph}_2$ derivative. These values are in the typical range for [Cp*Ru(diphosphine)(O_2)]$^+$ complexes,[49] and make these species formally Ru(IV)−peroxo complexes. Interestingly, all of the O−O stretching frequencies are within 9 cm^{-1}, and the O−O bond distances are the same within error. From these data it can be concluded that there is very little difference in the binding of O_2 with changes in the ligand. The conformation of the $P^R_2N^{R'}_2$ ligands in the peroxo species is identical to that in the chloride complexes, with the amine adjacent to the O_2 ligand positioned with its lone electron pair pointed away from the O_2 ligand.

The peroxo complex of the Cp derivative, [CpRu($P^{tBu}_2N^{Bn}_2$)(O_2)]$^+$, was obtained by reaction of [CpRu($P^{tBu}_2N^{Bn}_2$)]$^+$ with air but is not stable and could be isolated only in sufficient yield to obtain a crystal structure. Formation of the O_2 complex was observed on stirring a CD_2Cl_2 solution of [CpRu($P^{tBu}_2N^{Bn}_2$)]-[OTf], generated *in situ* from CpRu($P^{tBu}_2N^{Bn}_2$)Cl and TlOTf in air, forming a yellow solution in minutes. The peroxo complex was observed by NMR by the appearance of a singlet in the ^{31}P{^{1}H} NMR spectrum at 45.9 ppm, characteristically shifted upfield from the CpRu($P^{tBu}_2N^{Bn}_2$)Cl resonance (51.8 ppm). This peroxo complex decomposes completely over 1−2 h to an unidentified brown oil, and some decomposition is apparent even in the time required to prepare an NMR sample. Only one [CpRu(phosphine)$_2$(O_2)]$^+$ has been reported previously,[50] so instability is characteristic of these complexes. The high stability of the related Cl$^-$ and MeCN complexes suggests that the O_2

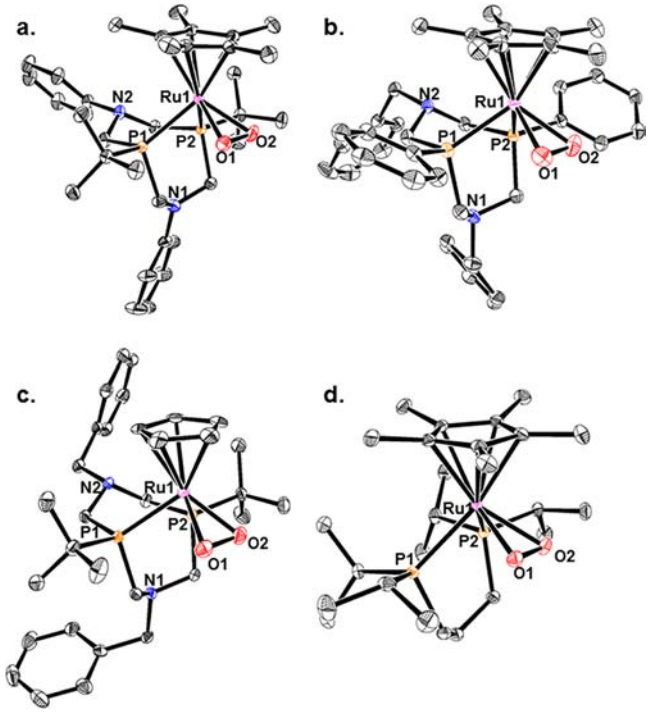

Figure 2. ORTEPs of (a) [Cp*Ru($P^{tBu}_2N^{Ph}_2$)(O_2)][BPh_4], (b) [Cp*Ru($P^{Ph}_2N^{Bn}_2$)(O_2)][OTf], (c) [CpRu($P^{tBu}_2N^{Bn}_2$)(O_2)][OTf], and (d) [Cp*Ru(dippp)(O_2)][PF_6]. Thermal ellipsoids are shown at 50% probability. Hydrogen atoms, counteranions, and solvent molecules have been omitted for clarity. Only one of the two independent molecules of [Cp*Ru(dippp)(O_2)][PF_6] in the unit cell are shown.

dx.doi.org/10.1021/ic3013987 | *Inorg. Chem.* 2012, 51, 10916−10928

ligand plays a role in the decomposition. Quickly layering a CH_2Cl_2 solution of $[CpRu(P^{tBu}{}_2N^{Bn}{}_2)(O_2)][OTf]$ with hexanes and storing the solution at −20 °C for weeks afforded a few X-ray quality crystals from which a structure was obtained. NMR spectra of these crystals were identical to the spectra of the compound prepared *in situ*. The X-ray crystal structure of $[CpRu(P^{tBu}{}_2N^{Bn}{}_2)(O_2)][OTf]$, to our knowledge the only crystal structure of a Cp ligated Ru−O_2 complex, is very similar to that of the Cp* complexes (Figure 2c, Table 2). The O_2 is bound η^2 with d(O1−O2) = 1.404(4) Å. While the esd on this distance is large, the similarity to the O−O bond distances of the Cp* derivatives is nonetheless striking considering the differences in the stability of these species and electron donating character of Cp* versus Cp (see electrochemical data and Table 4 below). From a simplistic perspective, a more electron donating Cp* ligand would be expected to give more peroxo character and a longer O−O distance, but this is not what is observed.[51] The solid state structure of $[CpRu(P^{tBu}{}_2N^{Bn}{}_2)(O_2)][OTf]$ contains a water molecule hydrogen-bonded to the O_2 ligand, with d(O2−O3) = 2.898(4) Å, which may impart stability to this structure and explain why it was able to be isolated despite the instability of solutions of this compound.

Protonation of Peroxo Complexes. *A. Effect of Phosphine Substituent on Protonation.* The ability of the pendent amines to direct protons to the O_2 ligand has been tested by adding acid to solutions of $[Cp^*Ru(P^R{}_2N^{R'}{}_2)(O_2)]^+$. We have reported previously that the *t*-butyl/benzyl derivative can be protonated at the pendent amine forming a stable complex $[Cp^*Ru(P^{tBu}{}_2N^{Bn}{}_2H)(O_2)]^{+2}$ in which there is an intramolecular hydrogen bond between the protonated amine and the O_2 ligand.[46] Protonation of $[Cp^*Ru(P^{Ph}{}_2N^{Bn}{}_2)(O_2)]^+$, which differs only in having a phenyl substituent at the phosphine, is very similar. Addition of 1 equiv of $[H^+DMF][OTf]$ to a CD_2Cl_2 solution of $[Cp^*Ru(P^{Ph}{}_2N^{Bn}{}_2)(O_2)][OTf]$ gives $[Cp^*Ru(P^{Ph}{}_2N^{Bn}{}_2H)(O_2)][OTf]_2$ by ^1H and ^{31}P NMR (eq 2). One benzylic resonance and the PCH_2N resonances of

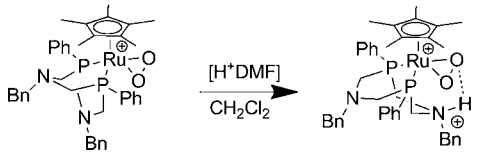

(2)

the ligand are shifted downfield, and a new, slightly broad singlet appears at 8.29 ppm in the ^1H NMR spectrum, consistent with protonation of one of the benzylamine ligands. Assignment of this new resonance at 8.29 ppm as the acidic benzylammonium proton is supported by the signal dropping in intensity when deuterium-labeled $[D^+DMF][OTf]$ is used to protonate $[Cp^*Ru(P^{Ph}{}_2N^{Bn}{}_2)(O_2)][OTf]$. The chemical shift of this benzylammonium is similar to the chemical shift of 7.68 ppm observed for protonated $[Cp^*Ru(P^{tBu}{}_2N^{Bn}{}_2H)(O_2)]^{+2}$, evidence that the environment of the acidic proton is similar between these two complexes. This chemical shift is inconsistent with the proton bridging the two benzylamine groups of the $P^{tBu}{}_2N^{Bn}{}_2$ ligand, since protons in such structures appear at ca. 15 ppm based on observations of protonated nickel−$P^R{}_2N^{Bn}{}_2$ complexes.[33] In the $^{31}P\{^1H\}$ NMR spectrum, a new sharp singlet resonance appears, shifted upfield by 5.4 ppm (Table 2). This upfield shift contrasts with the slight downfield shift and substantial broadening observed in $^{31}P\{^1H\}$ spectra upon protonation of $[Cp^*Ru(P^{tBu}{}_2N^{Bn}{}_2)(O_2)]^+$.[46]

$[Cp^*Ru(P^{Ph}{}_2N^{Bn}{}_2H)(O_2)]^{+2}$ is stable for days in solution and may be isolated as a red solid, similar to $[Cp^*Ru(P^{tBu}{}_2N^{Bn}{}_2H)(O_2)]^{+2}$. Red, X-ray quality crystals of $[Cp^*Ru(P^{Ph}{}_2N^{Bn}{}_2H)(O_2)][OTf]_2$ were obtained from an acetone solution of $[Cp^*Ru(P^{Ph}{}_2N^{Bn}{}_2)(O_2)][OTf]$ and $[H^+DMF][OTf]$ stored at −20 °C for one week. The X-ray structure obtained from these crystals suffers from multiply disordered triflate anions and acetone solvent, and is disordered in the position of the benzyl arms of the ligand (Figure 3). The

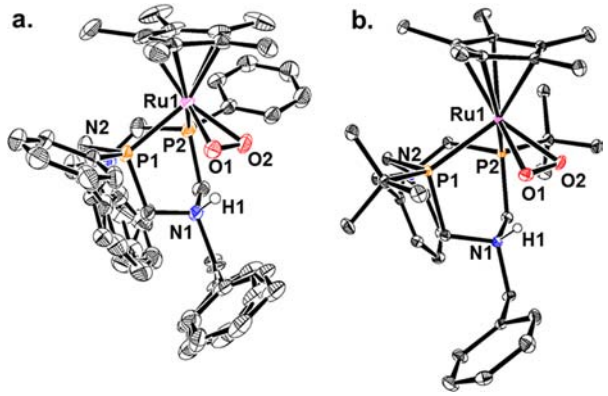

Figure 3. ORTEPs of (a) $[Cp^*Ru(P^{Ph}{}_2N^{Bn}{}_2H)(O_2)][OTf]_2\cdot$(acetone) and (b) $[Cp^*Ru(P^{tBu}{}_2N^{Bn}{}_2H)(O_2)][PF_6]_2\cdot(H_2O)_{0.25}$ (data from ref 46). Thermal ellipsoids are shown at 50% probability, except for benzyl groups of $[Cp^*Ru(P^{Ph}{}_2N^{Bn}{}_2H)(O_2)][OTf]_2$ for which both disordered groups are shown. Hydrogen atoms except for the acidic N−H, counteranions, and solvent molecules have been omitted for clarity. The acidic hydrogens were not located in the difference map, and were placed in geometrically idealized positions (a riding model).

thermal parameters of the disordered phenyl rings were restrained to be similar within each pair. However, no restraints were imposed that would have affected the structure of the complex other than the phenyl rings. The atomic positions of the core of the cationic portion of the molecule show clear evidence of protonation at the amine nearest the O_2 ligand, and there are strong similarities with the structure of $[Cp^*Ru(P^{tBu}{}_2N^{Bn}{}_2H)(O_2)]^{+2}$.[46] Both amines are inverted from their orientation in the unprotonated molecule, bringing nitrogen N1 within less than 2.9 Å from oxygen O2. This is characteristic of an NH···O hydrogen bond,[52] and bringing the lone pair of an amine within such a short distance of the lone pair of an O_2 ligand would be unlikely without protonation at the amine. The NH···O_2 interaction is asymmetric, with the protonated amine substantially closer to one oxygen atom than the other, d(N1···O2) = 2.716(4) Å, d(N1···O1) = 2.934(4) Å (Table 1).

The effect of varying the phosphine substituent on the basicity of $[Cp^*Ru(P^R{}_2N^{R'}{}_2)(O_2)]^+$ was tested by combining a CD_2Cl_2 solution of the protonated *t*-butylphosphine complex $[Cp^*Ru(P^{tBu}{}_2N^{Bn}{}_2H)(O_2)][PF_6]_2$ with an equimolar quantity of the unprotonated phenylphosphine compound $[Cp^*Ru(P^{Ph}{}_2N^{Bn}{}_2)(O_2)][OTf]$. ^1H and ^{31}P NMR spectra show distinct resonances of both the protonated and unprotonated forms of both the *t*-butyl- and phenyl-substituted complexes (eq 3,

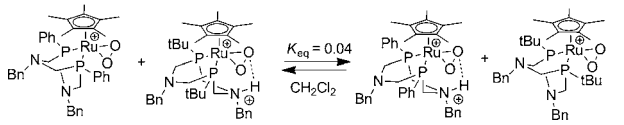

(3)

dx.doi.org/10.1021/ic3013987 | Inorg. Chem. 2012, 51, 10916−10928

Figure 4). Thus, proton exchange between the complexes is slow on the NMR time scale, and the equilibrium constant K_{eq}

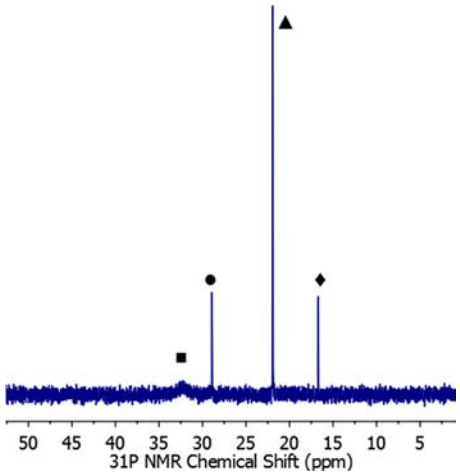

Figure 4. $^{31}P\{^1H\}$ NMR spectrum of the reaction of $[Cp^*Ru(P^{tBu}{}_2N^{Bn}{}_2H)(O_2)]^{+2}$ (■) with $[Cp^*Ru(P^{Ph}{}_2N^{Bn}{}_2)(O_2)]^{+}$ (▲) to form $[Cp^*Ru(P^{Ph}{}_2N^{Bn}{}_2H)(O_2)]^{+2}$ (♦) and $[Cp^*Ru(P^{tBu}{}_2N^{Bn}{}_2)(O_2)]^{+}$ (●) in CD_2Cl_2.

for this reaction is ~0.04 (based on integrations of the *t*-butyl and Cp* resonances in the ^1H NMR and of the $^{31}P\{^1H\}$ signals). From this it can be seen that the phosphine substituent, despite its distance from the amine in the $P^R{}_2N^{R'}{}_2$ ligand, exerts a measurable effect on the basicity of the complex, a difference in pK_a of ~1.4.

B. Effect of Amine Substituent on Protonation. Protonation of the *N*-phenyl derivative $[Cp^*Ru(P^{tBu}{}_2N^{Ph}{}_2)(O_2)][OTf]$ with 1 equiv of $[H^+DMF][OTf]$ to a CD_2Cl_2 solution also forms a protonated species. The NMR spectra of this complex indicate that protonation occurs at one pendent amine, likely the amine near the O_2, as for the complexes with pendent benzylamines. The sharp singlet in the $^{31}P\{^1H\}$ NMR spectrum of the unprotonated complex at δ = 30.2 ppm is shifted downfield by 11.5 ppm upon protonation. ^1H NMR spectra show a downfield shift of two of the PCH_2N and the aryl resonances, as well as the appearance of a broad singlet integrating to 1H at 9.98 ppm. This new broad singlet has been identified as a protonated pendent aniline by $^1H-^{15}N$ correlated NMR spectroscopy of isotopically labeled $[Cp^*Ru(P^{tBu}{}_2{}^{15}N^{Ph}{}_2)(O_2)][OTf]$. The 1D $^1H-^{15}N$ HSQC spectrum of $[Cp^*Ru(P^{tBu}{}_2{}^{15}N^{Ph}{}_2)(O_2)][OTf]$ with 1 equiv of $[H^+DMF][OTf]$ has one resonance at δ = 9.98 ppm, with a typical one-bond coupling constant, $J_{1H\text{-}15N}$ = 75 Hz. These data demonstrate protonation of the NPh group, and show that the proton does not bridge two anilines.[53,54]

Solutions of $[Cp^*Ru(P^{tBu}{}_2N^{Ph}{}_2H)(O_2)]^{+2}$ showed multiple decomposition products by NMR spectroscopy within a day. The stability of the protonated complexes is thus greatly reduced on decreasing the basicity of the pendent amine, since solutions of $[Cp^*Ru(P^{tBu}{}_2N^{Bn}{}_2H)(O_2)]^{+2}$ and $[Cp^*Ru(P^{Ph}{}_2N^{Bn}{}_2H)(O_2)]^{+2}$ showed no such signs of decomposition after several days at room temperature. While crystals of $[Cp^*Ru(P^{tBu}{}_2N^{Ph}{}_2H)(O_2)]^{+2}$ could not be obtained, IR spectra provide clear evidence for hydrogen bonding between the protonated pendent amine and the O_2 ligand. IR spectra of CH_2Cl_2 solutions of $[Cp^*Ru(P^{tBu}{}_2N^{Ph}{}_2)(O_2)]^{+}$ have an O–O stretch at 930 cm^{-1} ($\nu(^{18}O-^{18}O)$ = 880 cm^{-1}). Upon addition of 1 equiv of $[H^+DMF][OTf]$, this stretch is no longer present, but no new band is observed (see Supporting Information). Protonation of the $^{18}O_2$-labeled material shows a new band at 857 cm^{-1}, shifted −23 cm^{-1} from the band in the unprotonated material. A similar shift for the $^{16}O_2$ compound would place the stretch underneath a solvent absorption, explaining why the band was not observed. A ν(O–O) of ~910 cm^{-1} is predicted for the $^{16}O_2$ compound by a harmonic oscillator approximation, or a shift of ca. −20 cm^{-1} upon protonation. This shift in ν(O–O) is a little smaller than the −30 cm^{-1} observed on protonation of the related *N*-benzyl derivative $[Cp^*Ru(P^{tBu}{}_2N^{Bn}{}_2H)(O_2)][OTf]_2$.[46]

Density functional theory (DFT) calculations were performed to demonstrate that protonation at the aniline and hydrogen bonding to O_2 is a reasonable structure for this compound. Gas-phase geometry optimization of the unprotonated, cationic $[Cp^*Ru(P^{tBu}{}_2N^{Ph}{}_2)(O_2)]^{+}$ was performed at the BP86/6-31G** (C, H, N, O, P) SDD (Ru) level of theory on the singlet surface. This level of theory was chosen because of its previously demonstrated ability to reproduce the geometries of $[Cp^*Ru(P^{tBu}{}_2N^{Bn}{}_2)(O_2)]^{+}$and $[Cp^*Ru(P^{tBu}{}_2N^{Bn}{}_2H)(O_2)]^{+2}$.[46] The DFT optimized geometry of $[Cp^*Ru(P^{tBu}{}_2N^{Ph}{}_2)(O_2)]^{+}$ agrees well with the X-ray structure (see Table 3). A gas-phase optimization was also performed on the protonated $[Cp^*Ru(P^{tBu}{}_2N^{Ph}{}_2H)(O_2)]^{+2}$, which gave a minimum with the proton hydrogen bonding to the O_2 (Figure 5). The hydrogen bonding is asymmetric, with d(N1–O2) = 2.638 Å and d(N1–O1) = 2.998 Å. The calculated O–O stretching frequency is reduced on protonation by 20 cm^{-1}, which is quite consistent with experiment.

Table 3. Selected DFT-Calculated Bond Lengths and O–O Stretching Frequencies for $[Cp^*Ru(P^{tBu}{}_2N^{Ph}{}_2)(O_2)]^{+}$ and $[Cp^*Ru(P^{tBu}{}_2N^{Ph}{}_2H)(O_2)]^{+2}$[a]

	$[Cp^*Ru(P^{tBu}{}_2N^{Ph}{}_2)(O_2)]^{+}$ (diff from expt)	$[Cp^*Ru(P^{tBu}{}_2N^{Ph}{}_2H)(O_2)]^{+2}$
d(Ru–P)$_{avg}$ (Å)	2.411 (+0.039)	2.419
d(Ru–O1) (Å)	2.043 (+0.015)	2.044
d(Ru–O2) (Å)	2.050 (+0.027)	2.085
d(O1–O2) (Å)	1.404 (−0.002)	1.418
ν(O–O) (cm^{-1})	976 (+46)	956

[a]DFT calculations at the BP86/6-31G** (C, H, N, O, P) SDD (Ru) level of theory.

The change in the basicity of the complex on changing the pendent base was tested by NMR. A CD_2Cl_2 solution of the protonated *N*-phenyl complex, prepared *in situ* from $[Cp^*Ru(P^{tBu}{}_2N^{Ph}{}_2)(O_2)][OTf]$ and ca. 1 equiv of $[H^+DMF][OTf]$, was treated with ca. 1 equiv of $[Cp^*Ru(P^{tBu}{}_2N^{Bn}{}_2)(O_2)][OTf]$. Complete deprotonation of the aniline complex and formation of protonated benzylamine complex $[Cp^*Ru(P^{tBu}{}_2N^{Bn}{}_2H)(O_2)][OTf]_2$ was observed by ^1H and ^{31}P NMR. The relative integrations of the species in the product NMR spectra imply a difference in pK_a of at least ~3. The large difference is not surprising, given that the pK_a of aniline in acetonitrile is 6.3 pK_a units less than that of benzylamine.[55]

The complex $[Cp^*Ru(dippp)(O_2)][PF_6]$, without a pendent amine, does not protonate under the conditions tested. A CD_2Cl_2 solution showed no change in its NMR spectrum when 1 equiv of $[H^+DMF][OTf]$ was added. The O_2 ligand in this

dx.doi.org/10.1021/ic3013987 | *Inorg. Chem.* 2012, 51, 10916–10928

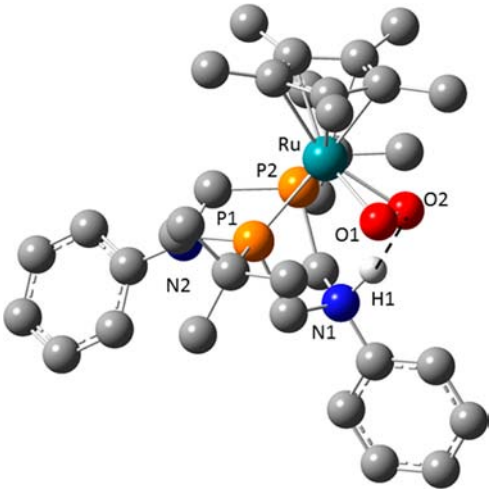

Figure 5. DFT (BP86/6-31G** (C, H, N, O, P) SDD (Ru)) optimized geometry of $[Cp^*Ru(P^{tBu}{}_2N^{Bn}{}_2H)(O_2)]^{+2}$. Hydrogen atoms except the acidic hydrogen have been omitted for clarity. The hydrogen bonding N1−H1···O2 interaction is indicated by a dashed line to H1.

complex, despite being formally reduced to a peroxide, is still less basic than dimethylformamide.

Electrochemical Characterization of $CpR''Ru(P^R{}_2N^{R'}{}_2)^+$ Complexes. *A. Oxidation of Chloride Complexes.* Cyclic voltammograms (CVs) of all of the chloride complexes show a reversible oxidation wave between −0.1 and −0.4 V versus $Cp_2Fe^{+/0}$, with typical peak separations of 0.12−0.15 V in CH_2Cl_2 with 0.1 M tetra-*n*-butylammonium hexafluorophosphate ($TBAPF_6$). The $E_{1/2}$ potentials are given in Table 4, and

Table 4. Half-Wave Potentials ($E_{1/2}$) for 1e$^-$ Oxidation of Chloride Complexes from CVs in CH_2Cl_2 (0.1 M $TBAPF_6$)

	$E_{1/2}$ vs $Cp_2Fe^{+/0}$ (V)[a]
$Cp^*Ru(P^{tBu}{}_2N^{Bn}{}_2)Cl$	−0.38
$Cp^*Ru(P^{Ph}{}_2N^{Bn}{}_2)Cl$	−0.38
$Cp^*Ru(P^{tBu}{}_2N^{Ph}{}_2)Cl$	−0.30
$CpRu(P^{tBu}{}_2N^{Bn}{}_2)Cl$	−0.12
$Cp^*Ru(dippp)Cl$	−0.40
$Cp^*Ru(P^{tBu}{}_2N^{Bn}{}_2)Cl + H^+DMF$	+0.22

[a]Estimated error in $E_{1/2}$ is ±0.01 V.

CVs are shown in the Supporting Information. The potentials show only modest differences with ligand, with all Cp* derivatives being within 0.1 V. The oxidation waves are attributed to $Ru^{II} \rightarrow Ru^{III}$ oxidation. To confirm this assignment, $Cp^*Ru(P^{tBu}{}_2N^{Bn}{}_2)Cl$ was chemically oxidized by 1 equiv of $[Cp_2Fe^+][PF_6^-]$ in CH_2Cl_2, yielding dark green crystals. The X-ray crystal structure (Figure S16 in the Supporting Information) confirms the composition as the Ru(III) complex $[Cp^*Ru(P^{tBu}{}_2N^{Bn}{}_2)Cl][PF_6]$ with no ligand oxidation. The Ru−Cl bond length (average of two independent molecules in the unit cell) is 0.115 ± 0.005 Å shorter in the Ru^{III} species than the parent Ru^{II} complex.

Cyclic voltammetry was also performed on a solution of $Cp^*Ru(P^{tBu}{}_2N^{Bn}{}_2)Cl$ in the presence of 1 equiv of $[H^+DMF][OTf]$. With the complex protonated, the wave corresponding to neutral $Cp^*Ru(P^{tBu}{}_2N^{Bn}{}_2)Cl$ oxidation is no longer present. Instead, a new reversible wave is observed, which is shifted from the complex in the absence of acid by +0.60 V.

B. Reduction of Dioxygen Complexes. CVs of the peroxo complexes $[Cp^*Ru(P^R{}_2N^{R'}{}_2)(O_2)]^+$ and $[Cp^*Ru(dippp)(O_2)]^+$ in CH_2Cl_2 (ca. 1.5 mM, 0.1 M $TBAPF_6$) show one completely irreversible reduction wave at potentials negative of −1 V vs $Cp_2Fe^{+/0}$ (see Supporting Information), as previously shown for $[Cp^*Ru(P^{tBu}{}_2N^{Bn}{}_2)(O_2)]^+$.[46] CVs were recorded in CH_2Cl_2 rather than acetonitrile or other more polar solvents that are typically used for CV because the O_2 ligand is displaced in coordinating solvents like acetonitrile. The potentials of the peak cathodic currents (E_{pc}) depend on the ligand, with a span of 0.23 V.

In the presence of 1 equiv of $[H^+DMF][OTf]$, a new irreversible reduction wave is observed for all $[Cp^*Ru(P^R{}_2N^{R'}{}_2)(O_2)]^+$, with a positive shift in E_{pc} (Figure 6, Table

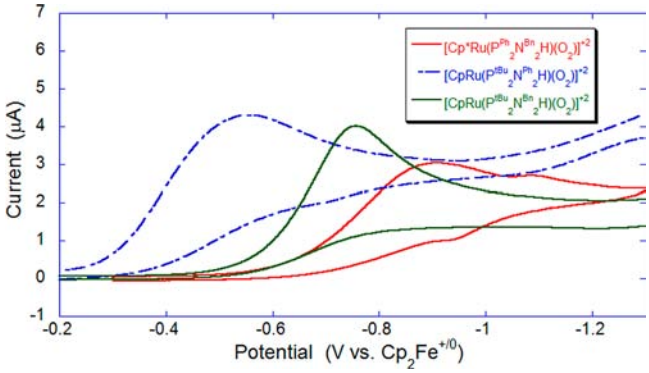

Figure 6. Overlay plot of reductive cyclic voltammograms of ca. 1.5 mM $[Cp^*Ru(P^{tBu}{}_2N^{Bn}{}_2)(O_2)][OTf]$ (green, solid), $[Cp^*Ru(P^{tBu}{}_2N^{Ph}{}_2)(O_2)][OTf]$ (blue, long dashes), and $[Cp^*Ru(P^{tPh}{}_2N^{Bn}{}_2)(O_2)][OTf]$ (red, solid) in CH_2Cl_2 (0.1 M $TBAPF_6$) in the presence of 1 equiv of $[H^+DMF][OTf]$. Scan rate is 0.1 V/s.

Table 5. Peak Irreversible Reduction Potentials (E_{pc}, V) from Cyclic Voltammograms of $[Cp^*Ru(diphosphine)(O_2)]^+$ in CH_2Cl_2 with and without Acid[a]

	E_{pc}	E_{pc} with 1 equiv $[H^+DMF][OTf]$	ΔE_{pc} (V)
$[Cp^*Ru(P^{tBu}{}_2N^{Bn}{}_2)(O_2)]^+$	−1.44	−0.77	+0.67
$[Cp^*Ru(P^{Ph}{}_2N^{Bn}{}_2)(O_2)]^+$	−1.55	−0.90	+0.65
$[Cp^*Ru(P^{tBu}{}_2N^{Ph}{}_2)(O_2)]^+$	−1.32	−0.56	+0.76
$[Cp^*Ru(dippp)(O_2)]^+$	−1.45	−1.22	+0.23

[a]CVs with ca. 1.5 mM complex in CH_2Cl_2 with 0.1 M $[n\text{-}Bu_4N][PF_6]$. Potentials referenced to $Cp_2Fe^{+/0}$, with estimated errors ±0.02 V.

5). This wave does not shift in potential with the addition of up to 10 equiv of $[H^+DMF][OTf]$. The magnitude of the shift, ΔE_{pc} (Table 5), is approximately +0.7 V for all three cations.

CVs of $[Cp^*Ru(dippp)(O_2)][PF_6]$, which lacks a pendent amine, also show an irreversible reduction wave in the presence of 1 equiv of $[H^+DMF][OTf]$ (Figure 7). Even though $[Cp^*Ru(dippp)(O_2)][PF_6]$ does not react with $[H^+DMF][OTf]$ (see above), this wave is shifted positive of the wave in the absence of acid. However, the magnitude of this shift (+0.23 V) is significantly smaller than for pendent amine complexes, suggesting that the pendent amine does play a role in facilitating reduction. The CV of $[Cp^*Ru(dippp)(O_2)][OTf]$ with $[H^+DMF][OTf]$ does appear to be qualitatively

dx.doi.org/10.1021/ic3013987 | Inorg. Chem. 2012, 51, 10916−10928

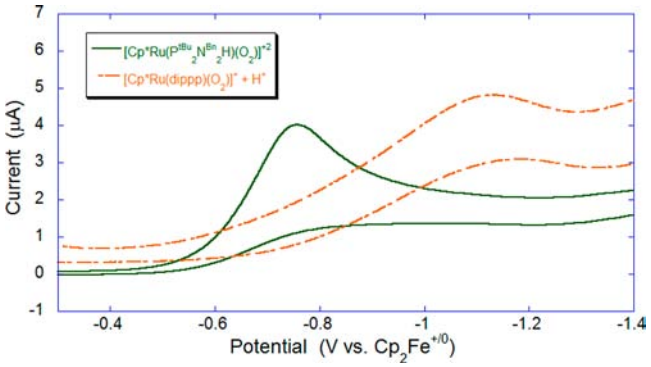

Figure 7. Overlay plot of reductive cyclic voltammograms of ca. 1.5 mM $[Cp^*Ru(P^{tBu}_2N^{Bn}_2)(O_2)][OTf]$ (green, solid) and $[CpRu(dippp)(O_2)][PF_6]$ (orange, dashed) in CH_2Cl_2 (0.1 M $TBAPF_6$) in the presence of 1 equiv of $[H^+DMF][OTf]$. Scan rate is 0.1 V/s.

somewhat different than for the $P^R_2N^{R'}_2$ complexes, with a much greater potential difference between the onset of cathodic current and the peak cathodic current E_{pc}, so this conclusion must be treated with some caution. The shape and position of this wave are not significantly affected by additional acid up to 10 equiv.

Cyclic voltammograms of $[Cp^*Ru(P^R_2N^{R'}_2)(O_2)]^+$ under an O_2 atmosphere in the presence of acid were also performed in order to test for O_2 reduction catalysis. Large catalytic currents were observed under these conditions. Unfortunately, these currents were also present at similar potentials in control experiments performed under identical conditions but in the absence of ruthenium complex. Thus, most of the current observed likely corresponded to direct O_2 reduction by the glassy carbon electrode at these very negative potentials (see Supporting Information).

To investigate the chemical processes occurring during reduction of the O_2 ligated complexes $[Cp^*Ru(P^R_2N^{R'}_2)(O_2)]^+$, reactions of these complexes with 4 equiv of Cp^*_2Fe ($E_{1/2}$ = −0.53 V vs Cp_2Fe)[56] were followed by NMR. Consistent with the E_{pc} potentials observed by CV, no reaction was observed in the absence of acid. Addition of 4 equiv of $[H^+DMF][OTf]$ to solutions of $[Cp^*Ru(P^R_2N^{R'}_2)(O_2)]^+$ and Cp^*_2Fe caused a rapid color change to bright green, indicating the formation of $[Cp^*_2Fe]^+$. The ^1H and ^{31}P NMR spectra of these reaction solutions contain a large number of peaks, none of which can be identified with certainty, but which suggest decomposition of the complex. With all the complexes, $^{31}P\{^1H\}$ NMR spectra showed downfield resonances in the +50 to +80 ppm range, suggestive of phosphine oxide formation, as well as resonances in the −50 to −20 ppm range suggestive of unbound phosphines.

Potential oxygen-atom acceptors were also reacted with the protonated complexes $[Cp^*Ru(P^R_2N^{R'}_2H)(O_2)]^{+2}$. As summarized in the Supporting Information, no reaction was observed with most substrates, including norbornene, thioanisole, and triphenylarsine. With the more basic phosphines, such as methyldiphenylphosphine, only deprotonation was observed.

DISCUSSION

Proton relays have been shown to be very valuable components of catalysts for the hydrogenase reaction, $2H^+ + 2e^- \rightleftharpoons H_2$, and are receiving increasing attention for other multielectron, multiproton processes.[22−46] While there has been much study of different $P^R_2N^{R'}_2$ ligands in nickel hydrogenase catalysis, the key parameters and design criteria for these ligands are only beginning to be understood. In this work, we have examined the effects of systematic variations in the of $[Cp^*Ru(P^R_2N^{R'}_2)]^+$ framework in the context of dioxygen reduction. Holding the other groups the same, the phosphorus substituent has been varied from *t*-butyl to phenyl, the nitrogen substituent has been changed from benzyl to phenyl, and the Cp* ligand has been replaced with Cp.

Substituting phenyl for *t*-butyl at the phosphine was expected to make the complexes less electron rich and therefore easier to reduce, due to the more electron-withdrawing character of the phenyl group. In previously studied $Ni(P^R_2N^{Ph}_2)_2$ complexes, substitution of phenyl for *n*-butyl resulted in changes in reduction potential ($\Delta E_{1/2}$'s) in acetonitrile of +0.09 V and +0.21 V for the Ni(II/I) and Ni(I/0) couples, respectively.[34] However, no difference was observed in CVs of the chloride complexes $Cp^*Ru(P^{tBu}_2N^{Bn}_2)Cl$ and $Cp^*Ru(P^{Ph}_2N^{Bn}_2)Cl$, and for the dioxygen complexes the *t*-butyl derivative $[Cp^*Ru(P^{tBu}_2N^{Bn}_2)(O_2)]^+$ is actually 0.11 V easier to reduce than the phenyl analogue (Tables 4 and 5). This may be due to a steric effect of the Cp* ring interacting with the *t*-butyl phosphines, hampering their ability to bind and donate to the Ru, as is reflected in the somewhat longer P−Ru bond distance for $Cp^*Ru(P^{tBu}_2N^{Bn}_2)Cl$ relative to $Cp^*Ru(P^{Ph}_2N^{Bn}_2)Cl$ (Table 1). A larger effect is observed upon substitution of Cp for Cp*, with an increase in $E_{1/2}$ of +0.26 V. This value is exactly the same as the difference between ferrocene and pentamethylferrocene (CpCp*Fe) under similar conditions ($\Delta E_{1/2}$ = +0.259(3)[56]).

Surprisingly, the effect of changing the amine substituent from R′ = Bn to Ph is larger than that of changing the phosphine substituent on the oxidation potential of the chloride ligated species. $Cp^*Ru(P^{tBu}_2N^{Bn}_2)Cl$ is 0.08 V easier to oxidize than $Cp^*Ru(P^{tBu}_2N^{Ph}_2)Cl$ (Table 4). A dependence of the redox potential of the metal center on the basicity of the pendent amine with $P^R_2N^{R'}_2$ has previously been demonstrated for $Ni(P^R_2N^{R'}_2)^{+2}$ complexes,[36] with $\Delta E_{1/2}$'s for R′ = *t*-butyl versus phenyl of +0.10 V and +0.17 V for the Ni(II/I) and Ni(I/0) couples, respectively, of $Ni(P^{Ph}_2N^{R'}_2)^{+2}$ in acetonitrile.[35] Still, it is surprising that the amine substituent four bonds from the Ru could have a larger effect than the phosphine substituent two bonds from the Ru, especially considering the crystallographic similarity in phosphine binding between these *t*-butyl phosphine complexes. The oxidation potential of Cp*Ru(dippp)Cl, without a relay, is within error of those of the *N*-benzyl derivatives $Cp^*Ru(P^{tBu}_2N^{Bn}_2)Cl$ and $Cp^*Ru(P^{Ph}_2N^{Bn}_2)Cl$, supporting the suggestion that this complex is a good analogue electronically to the $P^R_2N^{R'}_2$ complexes.

Not only do the amine substituents affect the ruthenium redox potential, but also the phosphine substituents significantly affect the amine basicity. $[Cp^*Ru(P^{Ph}_2N^{Bn}_2)(O_2)]^+$ is 1.4 pK_a units less basic than $[Cp^*Ru(P^{tBu}_2N^{Bn}_2)(O_2)]^+$ despite having a more negative reduction potential. This may be due to an electron-withdrawing effect of the phenyl phosphine on the pendent benzylamine. The aniline-derived proton relay is substantially less basic than the benzylamine relay, as expected. However, as observed with other $P^R_2N^{R'}_2$ complexes,[35] this change in basicity by several pK_a units was coupled to a change in redox potential of the complex of ca. 0.1 V (Table 5). These results show that the metal and its first coordination sphere are significantly coupled to the proton relays in the second

dx.doi.org/10.1021/ic3013987 | *Inorg. Chem.* 2012, 51, 10916−10928

coordination sphere. It is difficult to independently tune properties of a complex and its pendent proton relays.

The nature of the peroxo compounds $[Cp^*Ru(P^R_2N^{R'}_2)(O_2)]^+$ does not appear to be significantly affected by changes in the phosphine, aniline, or Cp groups, on the basis of the structural and spectroscopic parameters. This is surprising, as it might be expected on the basis of the electrochemical data obtained for the Cl^- and O_2 complexes that $[Cp^*Ru(P^{tBu}_2N^{Ph}_2)(O_2)][BPh_4]$ would be more easily reduced than $[Cp^*Ru(P^{tBu}_2N^{Bn}_2)(O_2)][BPh_4]$, and therefore would not donate as much electron density to the bound O_2, resulting in a shorter O−O bond. Substituting Cp for Cp* produced a complex with much lower stability, but this does not appear to be due to changes in Ru−O_2 bonding given the similarity of the X-ray structures. The reduced stability could be a steric effect, perhaps involving intermolecular reactions between Cp complexes that are not possible with the less accessible Cp* complexes.

Recent DFT calculations of Ru−polypyridyl water oxidation catalysts indicate that Ru(IV) η^1-peroxo species can be quite similar in energy to their η^2-peroxo analogues.[57,58] We have therefore calculated the energies of singlet and triplet η^1-peroxo $[Cp^*Ru(P^{tBu}_2N^{Bn}_2)(O_2)]^+$.[59,60] In the optimized geometries for both spin states (Figure S26 of the Supporting Information), the calculated O−O bond lengths are quite short (1.304 and 1.317 Å for the singlet and triplet, respectively). The calculated energies of these species (E − ZPE) are both 12 kcal mol^{-1} higher than the energy previously determined for the singlet η^2-peroxo species.[46] These findings are consistent with a recent, more thorough computational study of O_2 binding to CpRu(II) with different ligands, which also found η^1 species to be at higher energy (although in this study the η^1 triplet species were typically much lower in energy than the η^1 singlet).[61]

Protonation of the peroxo complexes $[Cp^*Ru(P^R_2N^{R'}_2)(O_2)]^+$ proceeds in essentially the same manner for all the compounds tested, despite the large differences in the basicities of the pendent amines and in the overall complexes. The proton is located on the amine near the O_2 ligand, forming a hydrogen bond to one of the O atoms in the O_2. The hydrogen bond should be stronger to a protonated pendent aniline versus a protonated pendent benzylamine because of the better pK_a matching between the aniline and the bound O_2. This is observed in the O···H−N hydrogen bonding distances predicted by DFT, with d(O2···N1) calculated to be 0.016 Å shorter for the aniline compound (Table 3). The hydrogen bond in $[Cp^*Ru(P^R_2N^{R'}_2H)(O_2)]^{+2}$ imparts a small amount of η^1-hydroperoxo character to the bound O_2 ligand, as can be seen by X-ray and in the DFT structures in the lengthening of the Ru−O bond to the hydrogen bonded O atom relative to the other Ru−O bond. Bonding to the positively charged H^+ pulls some electron density out of the Ru and onto the O_2. The additional electron density from Ru is donated to the O_2 π^* orbital, slightly weakening the O−O π bond. This is reflected in lower energy O−O bond stretching frequencies and longer bond lengths on protonation. It is therefore somewhat unexpected that the complex with the pendent aniline has a smaller shift in O−O stretching frequency upon protonation (~20 cm^{-1} versus 30 cm^{-1} for the benzylamine complex), despite forming an apparently stronger hydrogen bond. DFT calculations agree with this experimentally observed difference in O−O stretching frequency, predicting a shift of 20 cm^{-1} for the aniline complex versus 25 cm^{-1} for the benzylamine complex.[46] These calculations show that the O−O stretching vibration of the protonated species also involves motion of the $P^R_2N^{R'}_2$ ligand. Differences in the rigidity of the pendent aniline versus the pendent benzylamine may explain the differences in the shift in stretching frequency.

Protonation of the pendent amine substantially facilitates reduction of the peroxo complexes $[Cp^*Ru(P^R_2N^{R'}_2)(O_2)]^+$, as the cathodic peak potentials E_{pc} shift by 0.65−0.76 V (Table 5). The waves in the CVs are irreversible, which complicates the interpretation of these values. Still, the similarity between the complexes studied suggests that the ΔE_{pc} values may be reasonably compared. Some of the shift in E_{pc} is due to the additional positive charge on the complex, but this alone is unlikely to account for all of the ~0.7 V shift. The shift in the $Ru^{II/III}$ couple of $Cp^*Ru(P^{tBu}_2N^{Bn}_2)Cl$ in the presence and absence of acid of +0.60 V gives an approximate value for how the potential might shift due purely to the additional charge of the proton. This is not a perfect model because different electrochemical processes are being compared. However, each electrochemical process involves the interconversion of a monocation with a dication in the presence of protons, so the comparison is not unreasonable. The Coulombic effect of a proton at the pendent amine on the Ru center should be quite similar between the Cl^- and O_2 complexes. From this comparison it may be concluded that roughly +0.6 V of the shift for the O_2 complexes is due to the additional charge of the proton, and +0.1 V can be attributed to the reductions being proton-coupled processes.

It is probable that the first electron transferred occurs with proton transfer, producing a Ru(III) hydroperoxo complex. The protonated formally Ru(IV) η^2-peroxo complexes appear structurally primed to form such $Ru^{III}OOH$ species, which would be analogous to the isolated ruthenium(III) chloride compound $[Cp^*Ru(P^{tBu}_2N^{Bn}_2)Cl][PF_6]$. The dependence of ΔE_{pc} on the nature of the pendent amine is consistent with this proposal. ΔE_{pc} is 0.09 V larger for the aniline complex than for the related benzyl-amine complex because aniline is the weaker base, making proton transfer from aniline to the peroxide ligand more thermodynamically favorable in the aniline complex. Still, this shift is smaller than would have been expected, since 0.09 V is equivalent to a change in K_{eq} for electron transfer (ET) of $10^{1.5}$ while aniline is $10^{6.3}$ less basic than benzylamine (6.3 pK_a units in MeCN[55]).

The importance of the proton relays is indicated by comparing the peak reduction potentials for the $[Cp^*Ru(P^R_2N^{R'}_2)(O_2)]^+$ complexes versus that of $[Cp^*Ru(dippp)(O_2)]^+$, which does not contain a pendent amine. Protons do facilitate this reduction, but give a ΔE_{pc} of only 0.23 V, only about a third of the shift for the compounds with the proton relays. It is interesting that $[H^+DMF][OTf]$ does not protonate the O_2 ligand in the dippp complex (since the NMR spectra are unaffected by this acid). The O_2 ligand has very low basicity, suggesting that the Ru−O_2 interaction is quite covalent, so an ionic Ru(IV)−peroxide picture of these species is not accurate. From another perspective, the lack of protonation indicates that the dicationic Ru(IV) hydroperoxide is a high energy species. This analysis also illustrates the value of the proton relays, in holding protons close to a ligand with low basicity.

Despite the favorable interaction between the protonated pendent amine and the O_2, these complexes are not effective catalysts for O_2 reduction. Reduction of the peroxo complexes, both protonated and not, is completely irreversible, and the nature of the chemical processes occurring upon reduction is not known. The lack of anodic current in the CVs suggests a

rapid loss of ligand, either O_2 or phosphine, or rapid decomposition. For the unprotonated compounds, the control complex $[Cp^*Ru(dippp)(O_2)][PF_6]$ shows a similar irreversible wave at a similar potential, so the relays are not key to the decomposition. We have been unable to identify any of the products of reduction of $[Cp^*Ru(P^R{}_2N^{R'}{}_2)(O_2)]^+$ with acid, but ^{31}P NMR spectra of reductions with $Cp^*{}_2Fe$ are highly suggestive of phosphine oxidation. The proposed Ru^{III}–OOH intermediate could undergo many undesirable reactions, including ligand oxidation to form a phosphine oxide, which has been proposed for these types of complexes.[49e,62] The stabilization of this possible hydroperoxo intermediate by the pendent amine does not appear to be strong enough to prevent this phosphine oxidation reaction from occurring. Phosphine oxidation has been observed previously in O_2 reduction with $Ni(P^R{}_2N^{R'}{}_2)^{+2}$ complexes,[45] and remains a significant challenge for the use of $P^R{}_2N^{R'}{}_2$ ligands even for these relatively substitutionally inert species in the presence of oxidizing species. These results contrast with those of related ruthenium–nickel *thiolate* complexes $(L)Ru(NiS_2N_2)$ (L = Cp* or η^6-C_6Me_6, S_2N_2 is a dithiolate, diamine ligand).[63] These species bind O_2 to form stable ruthenium(IV)–peroxo species, and the hexamethylbenzene derivative is an active and stable ORR catalyst that has been used in a molecular fuel cell.[63c,d]

CONCLUSIONS

A series of Cp*Ru complexes with $P^R{}_2N^{R'}{}_2$ ligands has been prepared. All of the $[Cp^*Ru(P^R{}_2N^{R'}{}_2)]^+$ complexes tightly bind O_2, partially reducing O_2 to give formally a peroxide ligand. The $[Cp^*Ru(P^R{}_2N^{R'}{}_2)(O_2)]^+$ complexes bind protons at the amine near the O_2 ligand, directing the proton to the O_2 ligand through a hydrogen bonding interaction. The same proton directing is seen despite large differences in the basicity of the pendent amines. These compounds thus allow a clear visualization of one potentially key role of second-sphere proton relays in the oxygen reduction reaction. The series of compounds was made in order to adjust the properties of the metal center, by varying the phosphine and Cp substituents, and independently the properties of the relays, by varying the amine substituents. However, it was found that the properties of the metal center and the relays are intertwined, with changes in phosphine substituents affecting the amine basicity and change in amine substituent affecting the Ru redox potential. The species formed upon reduction of the peroxo complexes are unstable, and decomposition prevents these complexes from acting as oxygen reduction catalysts. However, cyclic voltammetry has shown that the positioned protons significantly facilitate reduction of the peroxo complexes, perhaps by protonating the O_2 ligand upon reduction.

EXPERIMENTAL SECTION

General Considerations. All manipulations were carried out under a nitrogen atmosphere using standard glovebox and Schlenk techniques unless otherwise specified. Solvents and reagents, including ^{15}N-labeled aniline and $^{18}O_2$ gas (97 atom % ^{18}O), were purchased from Aldrich unless otherwise noted. 1,3-Bis(diisopropylphosphino)-propane (dippp) was purchased from Strem. CD_2Cl_2 was purchased from Cambridge Isotope Laboratories and dried over CaH_2 prior to use. $RuCl_3{\cdot}3H_2O$ was purchased from Pressure Chemical Company. $[Cp^*RuCl]_4$,[64] $Cp^*Ru(PPh_3)_2Cl$,[65] $CpRu(PPh_3)_2Cl$,[66] $[H^+DMF][OTf]$,[67] and the ligands $P^{tBu}{}_2N^{Ph}{}_2$[40] and $P^{Ph}{}_2N^{Bn}{}_2$[35] were prepared following literature procedures. $Cp^*Ru(P^{tBu}{}_2N^{Bn}{}_2)Cl$, $[Cp^*Ru(P^{tBu}{}_2N^{Bn}{}_2)(O_2)][PF_6]$, and $[Cp^*Ru(P^{tBu}{}_2N^{Bn}{}_2H)(O_2)][PF_6]_2$ were prepared as reported previously.[46] IR spectra were recorded using a Bruker Optics Tensor27 FTIR spectrometer at room temperature as KBr pellets or in CH_2Cl_2 solution between NaCl plates as indicated. NMR spectra were recorded at 298 K on Bruker AV300, AV500, or DRX500 spectrometers. ^1H NMR chemical shifts are reported versus TMS and referenced to residual solvent. ^{31}P NMR chemical shifts are reported relative to an 85% $H_3PO_{4\,(aq)}$ external standard. Mass spectra were recorded on a Bruker Autoflex II MALDI-TOF. Elemental analysis was performed by Atlantic Microlabs.

Syntheses. *$Cp^*Ru(P^{tBu}{}_2N^{Ph}{}_2)Cl$.* The ligand $P^{tBu}{}_2N^{Ph}{}_2$ (0.223 g, 0.54 mmol) was suspended in 30 mL of THF. A slurry of $[Cp^*RuCl]_4$ (0.145 g, 0.13 mmol) in 10 mL of THF was added over a period of 5 min. The dark orange solution was stirred at room temperature for 2 days. The solution was evaporated to dryness. The orange solid was redissolved in 3 mL of toluene, filtered through Celite, and stored at −20 °C for 2 days to give dark orange X-ray quality crystals of $Cp^*Ru(P^{tBu}{}_2N^{Ph}{}_2)Cl{\cdot}$(toluene). The toluene was removed under vacuum to give $Cp^*Ru(P^{tBu}{}_2N^{Ph}{}_2)Cl$ as an orange powder (0.200 g, 53% yield). NMR(CD_2Cl_2) ^1H: 7.21 (m, 4H, Ar-*H*), 6.94 (m, 4H, Ar-*H*), 6.76 (m, 2H, Ph-*H*), 4.36 (m, 2H, PCH_2N), 3.81 (m, 2H, PCH_2N), 3.51 (m, 2H, PCH_2N), 3.00 (m, 2H, PCH_2N), 1.68 (s, 15H, $CpCH_3$), 1.39 (3-line pattern, 18H, tBu-CH_3). $^{31}P\{^1H\}$: 44.0 (s). Anal. (Calcd) C 59.72 (59.51); H 7.54 (7.49); N 4.10 (4.08)

$Cp^*Ru(P^{Ph}{}_2N^{Bn}{}_2)Cl$. The ligand $P^{Ph}{}_2N^{Bn}{}_2$ (0.483 g, 1.0 mmol) was suspended in 30 mL of toluene. To this suspension was added $Cp^*Ru(PPh_3)Cl$ (0.796 g, 0.98 mmol) slurried in 30 mL of toluene. This mixture was refluxed for 10 min, at which time an orange solution was formed. The orange solution was further refluxed for 36 h. It was then cooled to room temperature and vacuum-dried to give an orange oil. The orange oil was triturated with hexanes and vacuum-dried three times to give a yellow-orange powder. This powder was collected by filtration and washed once with 10 mL of acetone and then five times with 5 mL of hexanes. The yellow-orange powder was dried under vacuum to give $Cp^*Ru(P^{Ph}{}_2N^{Bn}{}_2)Cl$ (0.408 g, 55% yield). X-ray quality crystals were obtained from CH_2Cl_2 layered with hexanes at −20 °C. NMR(CD_2Cl_2) ^1H: 7.60–6.93 (m, 20H, Ph-*H*), 4.06 (s, 2H, $PhCH_2N$), 3.63 (m, 2H, PCH_2N), 3.43 (m, 2H, PCH_2N), 3.42 6 (s, 2H, $PhCH_2N$), 3.10 (m, 2H, PCH_2N), 2.37 (m, 2H, PCH_2N), 1.29 (s, 15H, $CpCH_3$). $^{31}P\{^1H\}$: 31.0 (s). Anal. (Calcd) C 64.27(63.69); H 6.44(6.28); N 3.71(3.71).

$CpRu(P^{tBu}{}_2N^{Bn}{}_2)Cl$. The ligand $P^{tBu}{}_2N^{Bn}{}_2$ (0.500 g, 1.1 mmol) was dissolved in 30 mL of toluene. To this was added $CpRu(PPh_3)Cl$ (0.730 g, 0.98 mmol) slurried in 30 mL of toluene. This mixture was refluxed for 10 min, at which time an orange solution was formed. The orange solution was further refluxed for 36 h. It was then cooled to room temperature and vacuum-dried to give an orange oil. The orange oil was triturated with hexanes and vacuum-dried three times to give a yellow-orange powder. This powder was collected by filtration and washed three times with 10 mL of hexanes. The yellow-orange powder was dissolved in 5 mL of toluene, layered with 8 mL of hexanes, and stored at −20 °C for two days, forming a yellow solid. This solid was collected by filtration and dried under vacuum to give $CpRu(P^{tBu}{}_2N^{Bn}{}_2)Cl$ (0.452 g, 72% yield). NMR(CD_2Cl_2) ^1H: 7.32–7.18 (m, 10H, Ph-*H*), 4.64 (s, 5H, Cp-*H*), 3.68 (s, 2H, $PhCH_2N$), 3.61 (s, 2H, $PhCH_2N$), 3.37 (m, 2H, PCH_2N), 2.68 (m, 2H, PCH_2N), 2.53 (m, 2H, PCH_2N), 2.42 (m, 2H, PCH_2N), 1.03 (3-line pattern, 18H, tBu-CH_3). $^{31}P\{^1H\}$: 51.8 Anal. (Calcd) C 58.09 (57.80); H 7.04 (7.16); N 4.31 (4.35).

$Cp^*Ru(dippp)Cl$. To a solution of 1,3-bis(diisopropylphosphino)-propane (dippp) (0.250 g, 0.90 mmol) in 15 mL of THF was added $[Cp^*RuCl]_4$ (0.245 g, 0.23 mmol) slurried in 10 mL of THF. The mixture was stirred overnight, forming an orange solution. This solution was passed through a Celite plug while open to air to remove a small amount of dark, insoluble material, and then dried under vacuum to give a light orange powder. The orange powder was dissolved in 3 mL of toluene, layered with 5 mL of hexanes, and stored at −20 °C. On standing overnight, red crystals formed, as well as a small amount of black oil. The red crystals of $Cp^*Ru(dippp)Cl$ were isolated by filtration, with the black oil remaining on the glassware, and washed with hexanes, giving (0.120 g, 24% yield) of $Cp^*Ru(dippp)Cl$. NMR(CD_2Cl_2) (The proton NMR spectrum is complex due to ^1H

dx.doi.org/10.1021/ic3013987 | Inorg. Chem. 2012, 51, 10916–10928

and ^{31}P coupling and has not been fully assigned.) ^{1}H: 2.59 (m, 2H), 2.18 (m, 3H), 2.05 (m, 2H), 1.80 (m, 2H), 1.63 (s, 15H, CpCH_3), 1.57 (m, 1H), 1.24−1.18 (m, 24H, CH(CH_3)$_2$). ^{31}P{^{1}H}: 32.5 (s). Anal. (Calcd) C 54.99 (54.78); H 9.01 (8.93).

[CpRu(P$^{tBu}_2$N$^{Bn}_2$)(MeCN)][PF$_6$]. To a solution of Cp*Ru(P$^{Ph}_2$N$^{Bn}_2$)Cl (0.020 g, 0.03 mmol) in 2 mL of CH_2Cl_2 was added $TlPF_6$ (0.11 g, 0.03 mmol) in 2 mL of CH_2Cl_2. After 30 min, the solution was passed through Celite to remove TlCl, leaving a red solution. To this solution was added an excess (approximately 5 μL) of acetonitrile, resulting in an immediate color change to yellow. This solution was dried to a yellow oil under vacuum, redissolved in acetonitrile, and layered with diethyl ether. On standing for several days at −35 °C, large yellow crystals of [CpRu(P$^{tBu}_2$N$^{Bn}_2$)(MeCN)][PF$_6$]·(diethyl ether) were obtained. The ether could be removed under vacuum to give [CpRu(P$^{tBu}_2$N$^{Bn}_2$)(MeCN)][PF$_6$] (0.008 g, 32% yield). NMR-(CD_2Cl_2) ^{1}H: 7.32−7.27 (m, 8H, Ph-*H*), 7.16 (d, 2H, Ph-*H*), 4.84 (s, 5H, Cp-*H*), 3.70 (s, 4H, PhCH_2N), 3.06 (m, 2H, PCH_2N), 2.58−2.50 (m, 6H, PCH_2N), 2.24 (s, 3H, NCCH_3), 1.04 (3-line pattern, 18H, tBu-CH_3) ^{31}P{^{1}H}: 52.6 (s), −144.0 (m, J^{19}F−^{31}P = 720 Hz). Anal. (Calcd) C 49.85 (49.87); H 6.23 (6.09); N 5.33 (5.29).

*[Cp*Ru(P$^{tBu}_2$N$^{Bn}_2$)Cl][PF$_6$].* To a solution of Cp*Ru(P$^{tBu}_2$N$^{Bn}_2$)Cl (0.100 g, 0.14 mmol) in 3 mL of CH_2Cl_2 was added a solution of ferrocenium hexafluorophosphate (0.046 g, 0.14 mmol) in 8 mL of CH_2Cl_2. The solution turned greenish-brown upon addition, and was stirred for an additional 20 min. The solution was vacuum-dried to a dark oil which was then triturated with 5 mL of toluene and filtered through paper, separating the dark green solid from the orange, ferrocene-containing filtrate. The green solid was then washed through the paper with 5 mL of acetone. The green liquid was layered with 5 mL of hexane and stored at −20 °C overnight, affording large green crystals of [Cp*Ru(P$^{tBu}_2$N$^{Bn}_2$)Cl][PF$_6$] (0.105 g, 87%). MS: (MALDI-TOF, pyrene matrix) 714.2 [M$^+$], 679.2 [M$^+$ − Cl]. Anal. (Calcd) C 50.49 (50.38); H 6.52 (6.34); N 3.32(3.26).

*[Cp*Ru(P$^{tBu}_2$N$^{Ph}_2$)(O$_2$)][OTf].* To an aerobic solution of Cp*Ru-(P$^{tBu}_2$N$^{Ph}_2$)Cl (0.053 g, 0.08 mmol) in 10 mL of acetone was added a solution of TlOTf (0.027 g, 0.08 mmol) in 5 mL of acetone. The yellow-orange solution immediately turned yellow-brown, and white TlCl precipitated. The solution was stirred for an additional 2 h, and then the TlCl was removed by filtration through a plug of Celite. The solution was dried to a brown oil under vacuum, triturated with hexanes, and dried again under vacuum to give [Cp*Ru(P$^{tBu}_2$N$^{Ph}_2$)-(O$_2$)][OTf] as a yellow-brown powder (0.059 g, 93%). X-ray quality crystals were obtained by evaporation of acetone solvent. NMR-(CD_2Cl_2) ^{1}H: 7.34 (m, 4H, Ar-*H*), 7.00 (m, 6H, Ar-*H*), 3.80 (m, 2H, PCH_2N), 3.74 (m, 2H, PCH_2N), 3.57 (m, 2H, PCH_2N), 3.24 (m, 2H, PCH_2N), 1.82 (s, 15H, CpCH_3), 1.48 (3-line pattern, 18H, tBu-CH_3). ^{31}P{^{1}H}: 30.2 (s). IR(KBr) ν(O−O) = 930 cm^{-1} [^{18}O = 880 cm^{-1}]. Anal. (Calcd) C 50.20 (50.47); H 6.20 (6.29); N 3.49 (3.36).

*[Cp*Ru(P$^{Ph}_2$N$^{Bn}_2$)(O$_2$)][OTf].* To an aerobic solution of Cp*Ru-(P$^{Ph}_2$N$^{Bn}_2$)Cl (0.070 g, 0.09 mmol) in 10 mL of acetone was added a solution of TlOTf (0.033 g, 0.09 mmol) in 5 mL of acetone. The yellow-orange solution immediately turned yellow-brown, and white TlCl precipitated. The solution was stirred for an additional 2 h, and then the TlCl was removed by filtration through a plug of Celite. The solution was dried to a brown oil under vacuum. This oil was recrystallized from acetone/hexanes at −20 °C for several days to give after filtration [Cp*Ru(P$^{Ph}_2$N$^{Bn}_2$)(O$_2$)][OTf]·(acetone) as a yellow-brown microcrystalline powder. The acetone could be removed *in vacuo* to give [Cp*Ru(P$^{Ph}_2$N$^{Bn}_2$)(O$_2$)][OTf] (0.065 g, 80%). X-ray quality crystals were obtained from CH_2Cl_2 layered with hexanes at −20 °C. NMR(CD_2Cl_2) ^{1}H: 7.79 (m, 4H, Ph-*H*), 7.59−7.43 (m, 12H, Ph-*H*), 6.93−6.85 (m, 4H, Ph-*H*), 4.06 (s, 2H, PhCH_2N), 3.63 (m, 2H, PCH_2N), 3.43 (m, 2H, PCH_2N), 3.42 6 (s, 2H, PhCH_2N), 3.10 (m, 2H, PCH_2N), 2.37 (m, 2H, PCH_2N), 1.29 (s, 15H, CpCH_3). ^{31}P{^{1}H}: 22.0 (s). IR(KBr) ν(O−O) = 926 cm^{-1} [^{18}O = 879 cm^{-1}]. Anal. (Calcd) for [Cp*Ru(P$^{Ph}_2$N$^{Bn}_2$)(O$_2$)][OTf]·(acetone) C 55.38 (55.11); H 5.62 (5.68); N 3.00 (2.92).

*[Cp*Ru(dippp)(O$_2$)][PF$_6$].* To an aerobic solution of Cp*Ru(dippp)Cl (0.075 g, 0.14 mmol) in 10 mL of acetone was added a solution of $TlPF_6$ (0.051 g, 0.15 mmol) in 5 mL of acetone. The orange solution immediately turned deep blue, and white TlCl precipitated. After 5 min of stirring open to air, the blue color changed to a light yellow, indicating formation of the O_2 complex. The solution was stirred for an additional 2 h, and then the TlCl was removed by filtration through a plug of Celite. The solution was dried to a brown oil under vacuum, triturated with hexanes, and dried again under vacuum to give [Cp*Ru(dippp)(O$_2$)][PF$_6$] as a brown powder (0.090 g, 93%). X-ray quality crystals were obtained from CH_2Cl_2 layered with hexanes at −20 °C. NMR(CD_2Cl_2) (The proton NMR spectrum is complex due to ^{1}H and ^{31}P coupling and has not been fully assigned.) ^{1}H: 2.55 (m, 2H), 2.48 (m, 1H), 1.96−1.89 (m, 6H), 1.77 (s, 15H, CpCH_3), 1.69 (m, 1H) 1.35 (m, 24H, CHCH_3). ^{31}P{^{1}H}: 23.5 (s), −144.0 (m, J^{19}F−^{31}P = 720 Hz). Anal. (Calcd) C 43.75 (43.54); H 7.35 (7.16).

X-ray Diffraction. Crystals were mounted on glass capillaries with Paratone-N oil (Hampton Research) and frozen immediately in a cold nitrogen gas stream at 100 K. X-ray diffraction data were collected on a Bruker APEXII single crystal diffractometer coupled to a Bruker APEXII CCD detector with graphite-monochromated Mo Kα radiation (λ = 0.710 73 Å). The data was integrated and scaled using SAINT, SADABS within the APEX2 software package by Bruker.[68] Solution by direct methods (SHELXS, SIR97[69]) produced a complete heavy atom phasing model consistent with the proposed structure. The structure was completed by difference Fourier synthesis with SHELXL97.[70,71] Scattering factors are from Waasmair and Kirfel.[72] All hydrogen atoms, including the hydrogen-bonding N−H protons, were placed in geometrically idealized positions and constrained to ride on their parent atoms with C−H and N−H distances in the range 0.90−1.00 Å (a riding model). Isotropic thermal parameters U_{eq} were fixed such that they were 1.2U_{eq} of their parent atom U_{eq} for CH's and NH's, and 1.5U_{eq} of their parent atom U_{eq} in the case of methyl groups. All non-hydrogen atoms were refined anisotropically by full-matrix least-squares. Collection and refinement data are presented in the Supporting Information. The structures of Cp*Ru(P$^{tBu}_2$N$^{Ph}_2$)Cl·(toluene) and [Cp*Ru(P$^{Ph}_2$N$^{Bn}_2$) (O$_2$)]-[OTf]·(hexane)$_{1/3}$·(CH$_2$Cl$_2$)$_{2/3}$ required restraints on the solvent molecules. The structures of [Cp*Ru(P$^{tBu}_2$N$^{Bn}_2$)Cl][PF$_6$]·(acetone)$_{1/2}$ and [CpRu(P$^{tBu}_2$N$^{Bn}_2$)(O$_2$)][OTf]·(CH$_2$Cl$_2$)$_2$·(H$_2$O) required restraints on the fluorines of the anions. The restraints used to fit the structure of [Cp*Ru(P$^{Ph}_2$N$^{Bn}_2$H)(O$_2$)][OTf]$_2$·(acetone) are described in the text.

Electrochemistry. Cyclic voltammetry (CV) was performed under N_2 using a CH Instruments 600D apparatus equipped with glassy carbon (1.0 mm diam) working electrode, glassy carbon rod auxiliary electrode, and Ag/Ag(NO)$_3$ (0.01 M in acetonitrile) reference electrode. CV was carried out in dichloromethane with 0.1 M [^{n}Bu$_4$N][PF$_6$] as supporting electrolyte. [^{n}Bu$_4$N][PF$_6$] was recrystallized three times from ethanol and dried under vacuum prior to use. Ferrocene or decamethylferrocene was added as internal standard, and all potentials are reported versus the $Cp_2Fe^{+/0}$ couple. In all cases, solutions were ca. 1−2 mM in concentration of Ru complex.

DFT Calculations. Calculations were performed with *Gaussian09*.[60] Geometry optimizations were performed in the gas phase on cations [Cp*Ru(P$^{tBu}_2$N$^{Bn}_2$)(η^1-O$_2$)]$^+$, [Cp*Ru(P$^{tBu}_2$N$^{Ph}_2$H)(O$_2$)]$^{+2}$, and [Cp*Ru(P$^{tBu}_2$N$^{Ph}_2$)(O$_2$)]$^+$. Calculations were performed with the BP86 functional, with the SDD basis set and effective core potential for Ru, and the 6-31G** basis set for all other atoms. Optimization of [Cp*Ru(P$^{tBu}_2$N$^{Ph}_2$)(O$_2$)]$^+$ was performed starting for the geometry of the crystal structure. All geometries were confirmed to be minima by vibrational analysis (NImag = 0).

■ ASSOCIATED CONTENT

Supporting Information

Additional NMR spectra, crystallographic refinement data and CIFs, IR spectra of O_2 complexes, cyclic voltammograms, DFT structure of [Cp*Ru(P$^{tBu}_2$N$^{Ph}_2$)(O$_2$)]$^+$, and coordinates of DFT optimized molecular geometries. This material is available free of charge via the Internet at http://pubs.acs.org

AUTHOR INFORMATION

Corresponding Author

*E-mail: mayer@chem.washington.edu.

Notes

The authors declare no competing financial interest.

ACKNOWLEDGMENTS

We thank Dr. John Roberts for assistance with electrochemical measurements, Dr. Johanna Blacquiere for help with mass spectrometry, and Dr. Mary Rakowski DuBois and Dr. Michael Mock for synthetic advice and helpful discussion. This work is supported as part of the Center for Molecular Electrocatalysis, an Energy Frontier Research Center funded by the U.S. Department of Energy, Office of Science, Office of Basic Energy Sciences.

REFERENCES

(1) Winter, M.; Brodd, R. J. *Chem. Rev.* **2004**, *104*, 4245.

(2) Borup, R.; Meyers, J.; Pivovar, B.; Kim, Y. S.; Mukundan, R.; Garland, N.; Myers, D.; Wilson, M.; Garzon, F.; Wood, D.; Zelenay, P.; More, K.; Stroh, K.; Zawodzinski, T.; Boncella, J.; McGrath, J. E.; Inaba, M.; Miyatake, K.; Hori, M.; Ota, K.; Ogumi, Z.; Miyata, S.; Nishikata, A.; Siroma, Z.; Uchimoto, Y.; Yasuda, K.; Kimijima, K.-I.; Iwishita, N. *Chem. Rev.* **2007**, *107*, 3904.

(3) Gewirth, A. A.; Thorum, M. S. *Inorg. Chem.* **2010**, *49*, 3557.

(4) Warren, J. J.; Tronic, T. A.; Mayer, J. M. *Chem. Rev.* **2010**, *110*, 6961.

(5) Savéant, J.-M. *Chem. Rev.* **2008**, *108*, 2348.

(6) Collman, J. P.; Boulatov, R.; Sunderland, C. J.; Fu, L. *Chem. Rev.* **2004**, *104*, 561.

(7) Shigehara, K; Anson, F. C. *J. Phys. Chem.* **1982**, *86*, 2776.

(8) Fukuzumi, S.; Okamoto, K.; Gros, C. P.; Guilard, R. *J. Am. Chem. Soc.* **2004**, *126*, 10441.

(9) Wisener, K.; Ohms, D.; Neumann, V.; Franke, R. *Mater. Chem. Phys.* **1989**, *22*, 457.

(10) Chang, C. J.; Deng, Y.; Shi, C.; Chang, C. K.; Anson, F. C.; Nocera, D. G. *Chem. Commun.* **2000**, 1355.

(11) Chang, C. J.; Loh, Z.-H.; Shi, C.; Anson, F. C.; Nocera, D. G. *J. Am. Chem. Soc.* **2004**, *126*, 10013.

(12) McCrory, C. C. L.; Ottenwaelder, X.; Stack, T. D. P.; Chidsey, C. E. D. *J. Phys. Chem. A* **2007**, *111*, 12641.

(13) McCrory, C. C. L.; Devadoss, A.; Ottenwaelder, X.; Lowe, R. D.; Stack, T. D. P.; Chidsey, C. E. D. *J. Am. Chem. Soc.* **2011**, *133*, 3696.

(14) Ward, A. L.; Elbaz, L.; Kerr, J. B.; Arnold, J. *Inorg. Chem.* **2012**, *51*, 4694.

(15) Fukuzumi, S.; Kotani, H.; Lucas, H. R.; Doi, K.; Suenobu, T.; Peterson, R. L.; Karlin, K. D. *J. Am. Chem. Soc.* **2010**, *132*, 6874.

(16) Kaila, V. R. I.; Verkhovsky, M. I.; Wikström, M. *Chem. Rev.* **2010**, *110*, 7062.

(17) Meunier, B.; de Visser, S. P.; Shaik, S. *Chem. Rev.* **2004**, *104*, 3947.

(18) Solomon, E. I.; Chen, P.; Metz., M.; Lee, S.-K.; Palmer, A. E. *Angew. Chem., Int. Ed.* **2001**, *40*, 4570.

(19) Collman, J. P.; Devaraj, N. K.; Decréau, R. A.; Yang, Y.; Yan, Y.-L.; Ebina, W.; Eberspacher, T. A.; Chidsey, C. E. D. *Science* **2007**, *315*, 1565.

(20) Shook, R. L.; Borovik, A. S. *Inorg. Chem.* **2010**, *49*, 3646.

(21) Collman, J. P.; Decréau, R. A.; Zhang, C. *J. Am. Chem. Soc.* **2004**, *69*, 3546.

(22) McGuire, R.; Dogutan, D. K.; Teets, T. S.; Suntivich, J.; Shao-Horn, Y.; Nocera, D. G. *Chem. Sci.* **2010**, *1*, 411.

(23) Dogutan, D. K.; Stoian, S. A.; McGuire, R.; Schwalbe, M.; Teets, T. S.; Nocera, D. G. *J. Am. Chem. Soc.* **2011**, *133*, 131.

(24) Shook, R. L.; Peterson, S. M.; Greaves, J.; Moore, C.; Rheingold, A. L.; Borovik, A. S. *J. Am. Chem. Soc.* **2011**, *133*, 5810.

(25) Carver, C. T.; Matson, B. D.; Mayer, J. M. *J. Am. Chem. Soc.* **2012**, *134*, 5444.

(26) DuBois, M. R.; DuBois, D. L. *Chem. Soc. Rev.* **2009**, *38*, 62.

(27) Small, Y. A.; DuBois, D. L.; Fujita, E.; Muckerman, J. T. *Energy Environ. Sci.* **2011**, *4*, 3008.

(28) Liu, T.; Chen, S.; O'Hagan, M. J.; DuBois, M. R.; Bullock, R. M.; DuBois, D. L. *J. Am. Chem. Soc.* **2012**, *134*, 6257.

(29) Lounissi, S.; Capon, J.-F.; Gloaguen, F.; Matoussi, F.; Pétillon, F. Y.; Schollhammer, P.; Talarmin, J. *Chem. Commun.* **2011**, *47*, 878.

(30) Camara, J. M.; Rauchfuss, T. B. *Nat. Chem.* **2012**, *4*, 26.

(31) Helm., M. L.; Stewart, M. P.; Bullock, R. M.; DuBois, M. R.; DuBois, D. L. *Science* **2011**, *333*, 863.

(32) Wiese, S.; Kilgore, U. J.; DuBois, D. L.; Bullock, R. M. *ACS Catal.* **2012**, *2*, 720.

(33) Wilson, A. D.; Shoemaker, R. K.; Miedaner, A.; Muckerman, J. T.; DuBois, D. L.; DuBois, M. R. *Proc. Natl. Acad. Sci. U.S.A.* **2007**, *104*, 6951.

(34) Kilgore, U. J.; Stewart, M. P.; Helm, M. L.; Dougherty, W. G.; Kassel, W. S.; DuBois, M. R.; DuBois, D. L.; Bullock, R. M. *Inorg. Chem.* **2011**, *50*, 10908.

(35) Fraze, K.; Wilson, A. D.; Appel, A. M.; DuBois, M. R.; Dubois, D. L. *Organometallics* **2007**, *26*, 3918.

(36) Kilgore, U. J.; Roberts, J. A. S.; Pool, D. H.; Appel, A. M.; Stewart, M. P.; DuBois, M. R.; Dougherty, W. G.; Kassel, W. S.; Bullock, R. M.; DuBois, D. L. *J. Am. Chem. Soc.* **2011**, *133*, 5861.

(37) Yang, J. Y.; Chen., S.; Dougherty, W. G.; Kassel, W. S.; Bullock, R. M.; DuBois, D. L.; Raugei, S.; Rousseau, R.; Dupuis, M.; DuBois, M. R. *Chem. Commun.* **2010**, *46*, 8618.

(38) Lee, C. H.; Dogutan, D. K.; Nocera, D. G. *J. Am. Chem. Soc.* **2011**, *133*, 8775.

(39) Jacobsen, G. M.; Yang, J. Y.; Twamley, B.; Wilson, A. D.; Bullock, R. M.; DuBois, M. R.; DuBois, D. L. *Energy Environ. Sci.* **2008**, *1*, 167.

(40) Wiedner, E. S.; Yang, J. Y.; Dougherty, W. G.; Kassel, W. S.; Bullock, R. M.; DuBois, M. R.; DuBois, D. L. *Organometallics* **2010**, *29*, 5390.

(41) Galan, B. R.; Schöffel, J.; Linehan, J. C.; Seu, C.; Appel, A. M.; Roberts, J. A. S.; Helm, M. L.; Kilgore, U. J.; Yang, J. Y.; DuBois, D. L.; Kubiak, C. P. *J. Am. Chem. Soc.* **2011**, *133*, 12767.

(42) Seu, C. S.; Appel, A. M.; Doud, M. D.; DuBois, D. L.; Kubiak, C. P. *Energy Environ. Sci.* **2012**, *5*, 6480.

(43) Weiss, C. J.; Groves, A. N.; Mock., M. T.; Dogherty, W. G.; Kassel, S. K.; Helm, M. L.; DuBois, D. L.; Bullock, M. R. *Dalton Trans.* **2012**, *41*, 4517.

(44) Mock, M. T.; Chen, S.; Rouseau, R.; O'Hagan, M. J.; Dougherty, W. G.; Kassel, W. S.; DuBois, D. L.; Bullock, R. M. *Chem. Commun.* **2011**, *47*, 12212.

(45) Yang, J. Y.; Bullock, R. M.; Dougherty, W. G.; Kassel, W. S.; Twamley, B.; DuBois, D. L.; DuBois, M. R. *Dalton Trans.* **2010**, *39*, 3001.

(46) Tronic, T. A.; DuBois, M. R.; Kaminsky, W.; Coggins, M. K.; Liu, T.; Mayer, J. M. *Angew. Chem., Int. Ed.* **2011**, *50*, 10936.

(47) Lin, W.; Wilson, S. R.; Girolami, G. S. *Organometallics* **1996**, *16*, 2987.

(48) Izutsu, K. *Acid–Base Dissociation Constants in Dipolar Aprotic Solvents*; Blackwell: Oxford, 1990.

(49) (a) Kirchner, K.; Mauthner, K.; Mereiter, K.; Schmid, R. *J. Chem. Soc., Chem. Comm.* **1993**, 892. (b) Mauthner, K.; Mereiter, K.; Schmid, R.; Kirchner, K. *Inorg. Chim. Acta* **1995**, *236*, 95. (c) Sato, M.; Asai, M. *J. Organomet. Chem.* **1996**, *508*, 121. (d) Lindner, E.; Haustein, M.; Fawzi, R.; Steimann, M.; Wegner, P. *Organometallics* **1994**, *13*, 5021. (e) Jia, G.; Ng, W. S.; Chu, H. S.; Wong, W.-T.; Yu, N.-T.; Williams, I. D. *Organometallics* **1999**, *18*, 3597. (f) de los Ríos, I.; Jiménez Tenorio, M.; Padilla, J.; Puerta, M. C.; Valerga, P. *Organometallics* **1996**, *15*, 4565.

(50) Palacios, M. D.; Puerta, M. C.; Valerga, P.; Lledós, A.; Veilly, E. *Inorg. Chem.* **2007**, *46*, 6958.

(51) (a) Praetorius, J. M.; Allen, D. P.; Wang, R.; Webb, J. D.; Grein, F.; Kennepohl, P.; Crudden, C. M. *J. Am. Chem. Soc.* **2008**, *130*, 3724.

(b) Covelli, D. *Probing the Electronic Structure of Dioxygen as a Ligand: Using X-Ray Absorption Spectroscopy to Quantify Backbonding*. Ph.D. Thesis, University of British Columbia, Vancouver, British Columbia, Canada, 2011.
(52) Jeffrey, G. A. *An Introduction to Hydrogen Bonding*; Oxford University Press: Oxford, U.K., 1997.
(53) Piertzak, M.; Stefaniak, L.; Pozharskii, A. F.; Ozeryanskii, V. A.; Nowicka-Scheibe, J.; Grech, E.; Webb, G. A. *J. Phys. Org. Chem.* **2000**, *13*, 35.
(54) Axenrod, T.; Pregosin, P. S.; Wieder, M. J.; Becker, E. D.; Bradley, R. B.; Milne, G. W. A. *J. Am. Chem. Soc.* **1971**, *93*, 6536.
(55) Kaljurand, I.; Kütt, A.; Sooväli, L.; Rodima, T.; Mäemets, V.; Leito, I.; Koppel, I. A. *J. Org. Chem.* **2005**, *70*, 1019.
(56) Noviandri, I.; Brown, K. N.; Fleming, D. S.; Gulyas, P. T.; Lay, P. A.; Masters, A. F.; Phillips, L. *J. Phys. Chem. B* **1999**, *103*, 6713.
(57) Concepcion, J. J.; Tsai, M.-K.; Muckerman, J. T.; Meyer, T. J. *J. Am. Chem. Soc.* **2010**, *132*, 1545.
(58) Lin, X.; Hu, X.; Concepcion, J. J.; Chen, Z.; Liu, S.; Meyer, T.; Yang, W. *Proc. Natl. Acad. Sci. U.S.A.* **2012**, *109*, 15669.
(59) Closed shell singlet and triplet η^1-peroxo species were located as minima by geometry optimization in the gas phase at the BP86/6-31G** (C, H, N, O, P) SDD (Ru) level of theory using *Gaussian09*.[60]
(60) Frisch, M. J.; et al. *Gaussian 09*. See Supporting Information for complete citation.
(61) Yu, H.; Fu, Y.; Guo, Q.; Lin, Z. *Organometallics* **2009**, *28*, 4443.
(62) Man, L. M.; Zhu, J.; Ng, S. M.; Zhou, Z.; Yin, C.; Lin, Z.; Lau, C. P. *Organometallics* **2004**, *23*, 6214.
(63) (a) Reynolds, M. A.; Rauchfuss, T. B.; Wilson, S. R. *Organometallics* **2003**, *22*, 1619−1625. (Addition: *Organometallics* **2003**, *22*, 4620.) (b) Canaguier, S.; Fontecave, M.; Artero, V. *Eur. J. Inorg. Chem.* **2011**, 1094−1099. (c) Kim, K.; Matsumoto, T.; Robertson, A.; Nakai, H.; Ogo, S. *Chem. Asian J.* **2012**, *7*, 1394−1400. (d) Matsumoto, T.; Kim, K.; Ogo, S. *Angew. Chem., Int. Ed.* **2011**, *50*, 11202−11205.
(64) Fagan, P. J.; Ward, M. D.; Calabrese, J. C. *J. Am. Chem. Soc.* **1989**, *111*, 1698.
(65) Boren, B. C.; Narayan, S.; Rasmussen, L. K.; Zhang, L.; Zhao, H.; Lin, Z.; Jia, G.; Fokin, V. V. *J. Am. Chem. Soc.* **2008**, *130*, 9823.
(66) Bruce, M. I.; Hameister, C.; Swincer, A. G.; Wallis, R. C. *Inorg. Synth.* **1982**, *21*, 78.
(67) Faviera, I.; Duñach, E. *Tetrahedron Lett.* **2004**, *45*, 3393.
(68) *Bruker APEX2 (Version 2.1-4), SAINT (Version 7.34A), SADABS (Version 2007/4)*; BrukerAXS Inc.: Madison, WI, 2007.
(69) (a) Altomare, A.; Burla, C.; Camalli, M.; Cascarano, L.; Giacovazzo, C.; Guagliardi, A.; Moliterni, A. G. G.; Polidori, G.; Spagna, R. *J. Appl. Crystallogr.* **1999**, *32*, 115. (b) Altomare, A; Cascarano, G; Giacovazzo, C; Guagliardi, A. *J. Appl. Crystallogr.* **1993**, *26*, 343.
(70) Sheldrick, G. M. *SHELXL-97, Program for the Refinement of Crystal Structures*; University of Göttingen: Göttingen, Germany, 1997.
(71) Mackay, S.; Edwards, C.; Henderson, A.; Gilmore, C.; Stewart, N.; Shankland, K.; Donald, A. *MaXus*; University of Glasgow: Glasgow, Scotland, 1997.
(72) Waasmaier, D.; Kirfel, A. *Acta Crystallogr., Sect. A* **1995**, *51*, 416.